

DC-DC CONVERTER FOR IOT DEVICES

By

Phoon Jun Hoe

A REPORT

SUBMITTED TO

Universiti Tunku Abdul Rahman

In fulfillment of the requirements

For the degree of

BACHELOR OF INFORMATION TECHNOLOGY(HONS) COMPUTER ENGINEERING

Faculty of Information and Communication Technology

Department of Computer and Communication Technology (Perak Campus)

**JAN 2017**

## REPORT STATUS DECLARATION FORM

**Title:** \_\_\_\_\_  
\_\_\_\_\_  
\_\_\_\_\_

**Academic Session:** \_\_\_\_\_

I \_\_\_\_\_  
(CAPITAL LETTER)

declare that I allow this Final Year Project Report to be kept in  
Universiti Tunku Abdul Rahman Library subject to the regulations as follows:

1. The dissertation is a property of the Library.
2. The Library is allowed to make copies of this dissertation for academic purposes.

Verified by,

\_\_\_\_\_  
(Author's signature)

\_\_\_\_\_  
(Supervisor's signature)

**Address:**

\_\_\_\_\_  
\_\_\_\_\_  
\_\_\_\_\_

\_\_\_\_\_  
Supervisor's name

**Date:** \_\_\_\_\_

**Date:** \_\_\_\_\_

DC-DC CONVERTER FOR IOT DEVICES

By

Phoon Jun Hoe

A REPORT

SUBMITTED TO

Universiti Tunku Abdul Rahman

In fulfillment of the requirements

For the degree of

BACHELOR OF INFORMATION TECHNOLOGY(HONS) COMPUTER ENGINEERING

Faculty of Information and Communication Technology

Department of Computer and Communication Technology (Perak Campus)

**JAN 2017**

## **DECLARATION OF ORIGINALITY**

I declare that this report entitled “DC-DC CONVERTER FOR IOT DEVICES” is my own work except as cited in the references. The report has not been accepted for any degree and is not being submitted concurrently in candidature for any degree or other award.

Signature : \_\_\_\_\_

Name : \_\_\_\_\_

Date : \_\_\_\_\_

## **ACKNOWLEDGEMENTS**

I would like to thank my supervisor for the continuous support and guidance for this project. A lot of knowledge about power electronics and MPPT have been obtained through the dealings with MOSFET. My supervisor advised me on problems I encountered and gave suggestions on how to solve or provide an alternative to tackle the problem.

I would also like to thank my peers in helping me record videos for demonstration purposes. The videos are of how the system works and how readings are obtained. Total of 3 days were used in video recording because of the unstable weather. My peers too give opinions towards the project and I appreciate them a lot.

## **ABSTRACT**

This project is about designing a highly efficient DC-DC converter for renewable energy source, solar energy. Using this energy, the designed DC-DC converter regulates and reduces the voltage of the fluctuating input to charge a battery for future use.

The efficiency is computed in real time using the input and output voltages and current. The power for both input and output is used to find the efficiency of this system. The system is self-sustainable as it uses renewable energy to power itself and at the same time charges the battery.

The system will be tested under sunlight to see its self-sustainability and how the microcontroller changes its duty cycle under different sunlight conditions to fit the input conditions for the battery.

# TABLE OF CONTENTS

<b>TITLE</b>	<b>i</b>
<b>DECLARATION OF ORIGINALITY</b>	<b>ii</b>
<b>ACKNOWLEDGEMENTS</b>	<b>iii</b>
<b>ABSTRACT</b>	<b>iv</b>
<b>TABLE OF CONTENTS</b>	<b>v</b>
<b>LIST OF FIGURES</b>	<b>vi</b>
<b>LIST OF TABLES</b>	<b>viii</b>
<b>LIST OF ABBREVIATIONS</b>	<b>ix</b>
<b>CHAPTER 1: INTRODUCTION</b>	
1.0 Project Motivation	<b>1</b>
1.1 Project Background	
1.1.1 DC-DC Converter and MPPT	<b>2</b>
1.2 Project Objective	<b>6</b>
1.3 Project Scope	<b>6</b>
<b>CHAPTER 2: LITERATURE REVIEW</b>	
2.0 Theoretical and Practical Study of a Photovoltaic MPPT Algorithm Applied to Voltage Battery Regulation.	<b>7</b>
2.1 A New Sensorless Hybrid MPPT Algorithm Based on Fractional Short-Circuit Current Measurement and P&O MPPT.	<b>8</b>
2.2 A Fast PV Power Tracking Control Algorithm With Reduced Power Mode.	<b>10</b>
<b>CHAPTER 3: SYSTEM DESIGN</b>	
3.0 Proposed Buck Converter	<b>11</b>
3.1 Simulation of Buck Converter	<b>14</b>

3.2 Selection of Microcontroller	17
3.2 Hardware and components required	20
3.3 Circuit Setup	22
3.4 Microcontroller coding setup	24
3.5 Pins and ports used in microcontroller	27
3.6 Features of the charger	29
3.7 Operation states of the charger	30
3.8 Auto-sleep feature	32
3.10 Specification of solar panel	33
3.11 Charging the battery	34

#### **CHAPTER 4: METHOD/TECHNOLOGIES INVOLVED**

4.0 Operation of Buck converter	35
4.1 Operation of MPPT algorithms	37

#### **CHAPTER 5: IMPLEMENTATION, TESTING AND ANALYSIS**

5.0 Verification Plan	43
5.1 Testing	44
5.2 Practical vs Theoretical efficiency comparison of Buck converter	47
5.3 Quantifying power and efficiency	
5.3.1 Power consumption of microcontroller	50
5.3.2 Requirements for MPPT	50
5.3.3 Efficiency with MPPT algorithm	50
5.3.4 Efficiency without MPPT algorithm	51
5.4 Power comparison between P&O, InC and No_MPPT	52
5.5 Analysis of MPPT algorithms and without MPPT algorithm	55
Summary of analysis	57
5.6 Issues and challenges	58
5.7 Solution to problem	58



5.8 Limitations	59
5.9 Timeline	60
<b>CHAPTER 6: CONCLUSION</b>	
6.0 Project Review	62
6.1 Further improvements in future	63
6.2 Final remark	64
<b>REFERENCES</b>	
<b>APPENDIX A Datasheet of IR2104</b>	<b>A-1</b>
<b>APPENDIX B Datasheet of IRFZ44N</b>	<b>B-1</b>
<b>APPENDIX C Datasheet of ATmega328</b>	<b>C-1</b>
<b>APPENDIX D Graph of Output Voltage versus Sensed Current of ACS712</b>	<b>D-1</b>

## LIST OF FIGURES

<b>Figure Number</b>	<b>Title</b>	<b>Page</b>
<i>Figure 1.1</i>	<i>The I-V and P-V characteristics curves of a PV module (Solar Panel)</i>	2
<i>Figure 1.1</i>	<i>Circuit diagram of a buck converter</i>	3
<i>Figure 1.2</i>	<i>Circuit diagram of a boost converter</i>	3
<i>Figure 1.3</i>	<i>Circuit diagram of an Inverting buck-boost converter</i>	4
<i>Figure 1.4</i>	<i>Circuit diagram of Non-Inverting buck-boost converter</i>	4
<i>Figure 1.5</i>	<i>Circuit diagram of SEPIC</i>	4
<i>Figure 2.1</i>	<i>The block diagram of the voltage charge regulator</i>	8
<i>Figure 2.2</i>	<i>Flowchart of the P&amp;O part of hybrid MPPT</i>	9
<i>Figure 2.3</i>	<i>Block diagram of the FSCC part of hybrid MPPT</i>	9
<i>Figure 2.4</i>	<i>Block diagram of the overall system</i>	10
<i>Figure 3.1</i>	<i>The circuit diagram for a synchronous buck converter</i>	11
<i>Figure 3.2</i>	<i>Typical connection of the IR2104</i>	12
<i>Figure 3.3</i>	<i>Function diagram of the IR2104</i>	13
<i>Figure 3.4</i>	<i>The simulation circuit for buck converter</i>	14
<i>Figure 3.5</i>	<i>The simulation result for the buck converter</i>	16
<i>Figure 3.6</i>	<i>Board view of the Arduino Uno</i>	18
<i>Figure 3.7</i>	<i>Circuit diagram of the Synchronous buck converter with microcontroller as the controller to find MPP</i>	22
<i>Figure 3.8</i>	<i>Circuit schematic of the Synchronous buck converter</i>	28
<i>Figure 3.10</i>	<i>The operation state diagram of the system</i>	31
<i>Figure 3.12</i>	<i>The 15W solar panel used for the system</i>	33
<i>Figure 4.1</i>	<i>Square wave with the duty cycle of 50% in the first period and duty cycle of 70% in the second period.</i>	35

<i>Figure 4.2</i>	<i>Buck converter operation during M1 on period</i>	36
<i>Figure 4.3</i>	<i>Buck converter operation during M1 off period</i>	36
<i>Figure 4.4</i>	<i>Flowchart for Perturb &amp; Observe algorithm</i>	38
<i>Figure 4.5</i>	<i>The I-V and P-V characteristics curves of a PV module (Solar Panel)</i>	39 30
<i>Figure 4.6</i>	<i>Flowchart of Incremental Conductance algorithm</i>	41
<i>Figure 5.2</i>	<i>The oscilloscope showing two pulse wave as verification</i>	44
<i>Figure 5.3</i>	<i>The physical diagram of the system with the battery connected</i>	45
<i>Figure 5.4</i>	<i>The LCD screen when the system is running</i>	46
<i>Figure 5.11</i>	<i>The P-T graph of 3 methods under partial shading condition for test case 1</i>	52
<i>Figure 5.12</i>	<i>The P-T graph of 3 methods under fully exposed condition for test case 1</i>	53
<i>Figure 5.13</i>	<i>The P-T graph of 3 methods under fully exposed condition for test case 2</i>	54
<i>Figure 5.14</i>	<i>The P-T graph of 3 methods under fully exposed condition for test case 3</i>	54

## LIST OF TABLES

<b>Table Number</b>	<b>Title</b>	<b>Page</b>
<i>Table 1.7</i>	<i>The properties of online and offline methods in finding MPP</i>	5
<i>Table 3.9</i>	<i>Different states' condition and description</i>	30
<i>Table 3.11</i>	<i>The solar panel's specification and characteristics</i>	33
<i>Table 5.1</i>	<i>Verification Plan for the system</i>	43
<i>Table 5.5</i>	<i>The efficiency of buck converter under different components and frequency</i>	47
<i>Table 5.6</i>	<i>Comparison of efficiency on varied frequency in terms of 100 uH inductor value</i>	48
<i>Table 5.7</i>	<i>Comparison of efficiency on varied frequency in terms of 10 uH inductor value</i>	48
<i>Table 5.8</i>	<i>The state of the charger corresponding to the backlight color of the LCD</i>	49
<i>Table 5.9</i>	<i>The power consumption of the microcontroller in different conditions</i>	50
<i>Table 5.10</i>	<i>The three test cases that have been made against these 3 charging methods.</i>	52
<i>Table 5.15</i>	<i>The detailed comparison of the three methods of charging tested for test case 1</i>	55
<i>Table 5.16</i>	<i>The detailed comparison of the three methods of charging tested for test case 2</i>	56
<i>Table 5.17</i>	<i>The detailed comparison of the three methods of charging tested for test case 3</i>	56

## LIST OF ABBREVIATIONS

<i>MPPT</i>	Maximum Power Point Tracking
<i>MPP</i>	Maximum Power Point
<i>FSCC</i>	Fractional Short-Circuit Current
<i>FOCV</i>	Fractional Open-Circuit Voltage
<i>LCD</i>	Liquid Crystal Display
<i>CLK</i>	Clock
<i>CPU</i>	Control Processing Unit
<i>INT</i>	Interrupt
<i>EEPROM</i>	Electrically Erasable Programmable Read Only Memory
<i>I/O</i>	Input/Output
<i>ASY</i>	Asynchronous
<i>WDT</i>	Watch Dog Timer
<i>P&amp;O</i>	Perturb and Observe
<i>InC</i>	Incremental Conductance
<i>SEPIC</i>	Single-ended Primary-Inductor Converter
<i>PV</i>	Photovoltaic
<i>PWM</i>	Pulse Width Modulation
<i>ADC</i>	Analog to Digital Converter
<i>MOSFET</i>	Metal Oxide Semiconductor Field Effect Transistor
<i>I2C</i>	Inter-interconnected Circuit
<i>UART</i>	Universal Asynchronous Receiver/Transmitter

<i>I</i>	Current
<i>V</i>	Voltage
<i>P</i>	Power
<i>LPM</i>	Low Power Mode
<i>USB</i>	Universal Serial Bus
<i>PC</i>	Personal Computer

## CHAPTER 1: INTRODUCTION

### 1.0 PROJECT MOTIVATION

In the way of going into the future, energy or power consumption plays a huge role in advancing technologically. Based on the statistics made by Global Energy Statistic Year Book (2015), energy consumption has increases approximately 400 Mtoe(Million Tonnes of Oil Equivalent) per year since the year 2000. In a way, consuming renewable energy is much more cost effective and indirectly helps plenty of operations in producing higher throughput by investing more money on the research and development and lesser on the cost needed for manufacturing or production. The idea is to use the energy from the sun or any other renewable energy power source to charge a portable charger (power bank) or battery. Therefore, the main focus of this project is to create a DC-DC converter to convert the higher input voltage from PV module or any renewable energy source into a lower voltage to the power bank or vice versa while maintaining the maximum power. This is necessary as the rated input of most power bank is between 5-5.2 V and to maintain a stress-free battery and longer battery life mentioned by Battery University (2016), the higher voltage must be stepped down by a buck converter to charge the portable charger. However, due to the fluctuating input voltage of PV module, adjustments are needed to be made in the control of buck converter. An algorithm is needed to track the maximum power point (MPP) to increase the efficiency of the converter. Figure 1.1 shows characteristic curve at one operating point where the MPP might change given the different environmental condition.

This system would be suitable commercially for everyone as people nowadays has gadgets such as smartphones, tablets, MP3 players etc. and all gadgets uses power. People would definitely prefer to have this system to charge their power bank without having to plug into a socket.

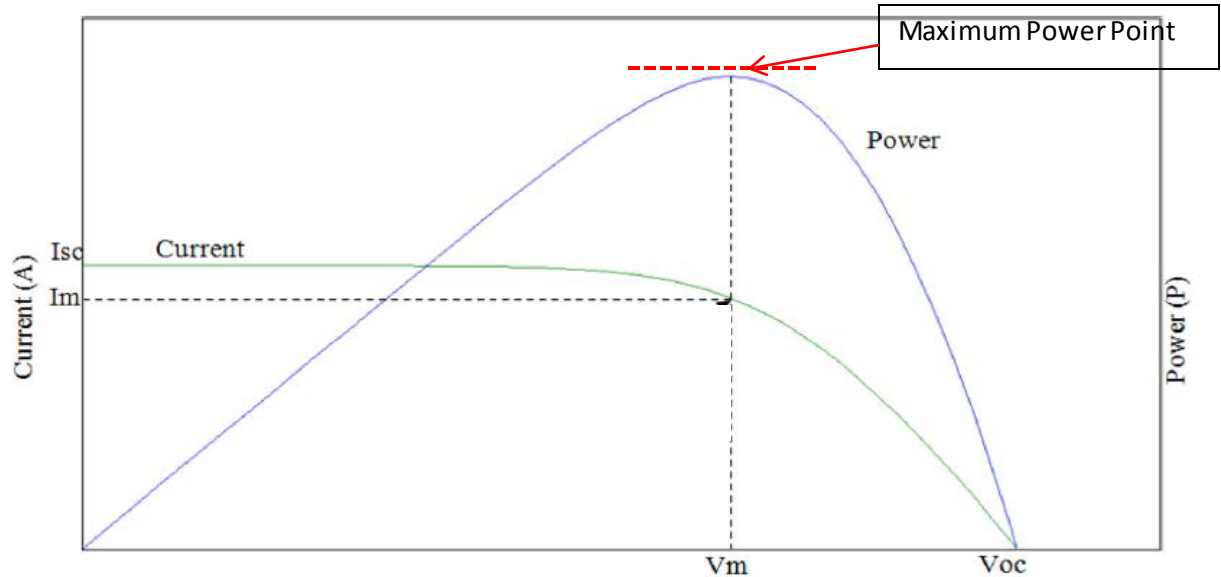


*Figure 1.1: The I-V and P-V characteristics curves of a PV module (Solar Panel) obtained from Simple and low cost incremental conductance maximum power point tracking using buck-boost converter (2013)*

## 1.1 PROJECT BACKGROUND

### 1.1.1 DC-DC Converter and MPPT

There are 4 common types of DC-DC converter; buck (Figure 2.1), boost (Figure 2.2), buck-boost and SEPIC Converter (Figure 2.5). If the input voltage is higher than the needed voltage for output, buck converter would be ideal as the number of components of the converter will be minimal and the efficiency can usually be more than 95% (Source Resistance: The Efficiency Killer in DC-DC Converter Circuits, 2004). If the input voltage is lower than the needed voltage for output, boost converter would be ideal as the number of components of the converter will also be minimal and the efficiency is very high.

The buck-boost and SEPIC can both be a step-up or step-down voltage converter as buck-boost is essentially a combination of buck and boost converter. There are 2 types of buck-boost converter where the difference is at the output voltage; Inverting buck-boost converter (Figure 2.2) where the output voltage is in the reverse direction of the input voltage and the Non-



Inverting buck-boost converter (Figure 2.3) where the output voltage is in the same direction as the input voltage.

SEPIC (Single-Ended Primary-Inductor Converter) is a boost converter followed by a buck-boost converter. However, SEPIC has numerous advantages over the buck-boost converter. First of all, the SEPIC is able to achieve the same output as buck-boost converter using lesser components than the non-inverting buck-boost converter and still produce a non-inverting voltage output. Keeping.S (2014) mentioned that the voltage inversion can add complexity to a design, particularly when supplying analog components. Furthermore, he states that the capacitor coupling energy from input to output allows the device to deal with short circuits in a more controlled manner than the traditional buck/boost design.

\*Circuits below are drawn by a circuit simulator

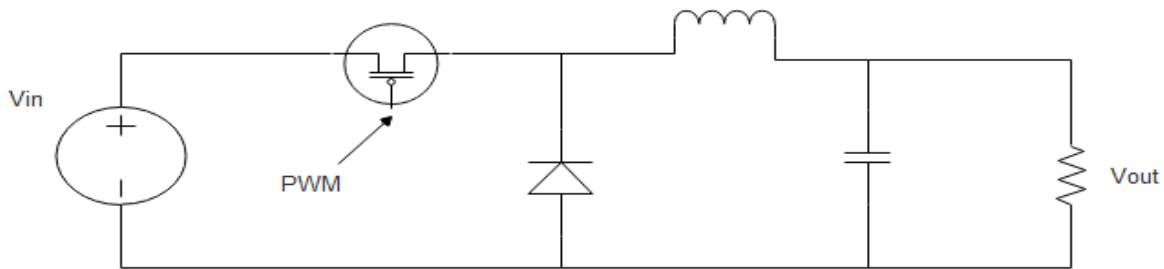


Figure 1.2: Circuit diagram of a buck converter (Switched Mode Power Supplies, p 4)

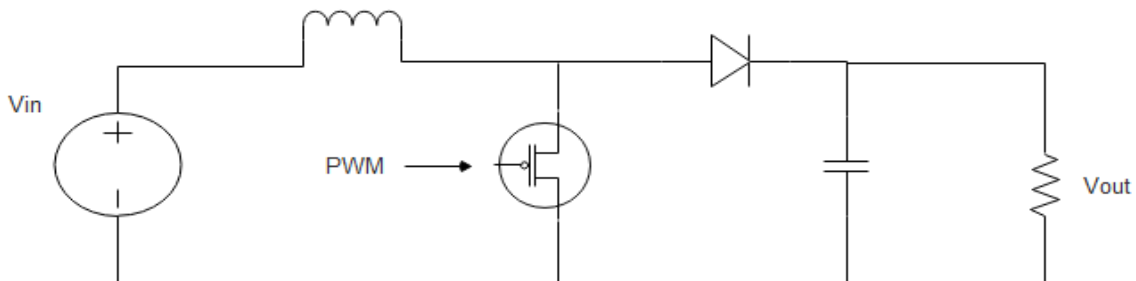


Figure 1.3: Circuit diagram of a boost converter (Switched Mode Power Supplies, p 7)

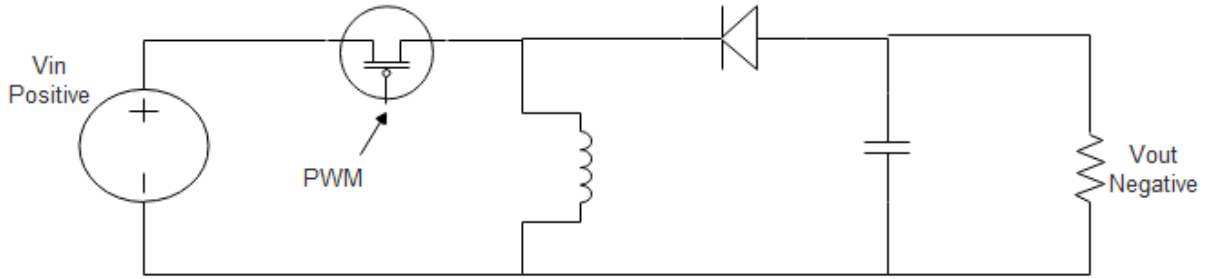


Figure 1.4: Circuit diagram of an Inverting buck-boost converter (Keeping. S, 2014)

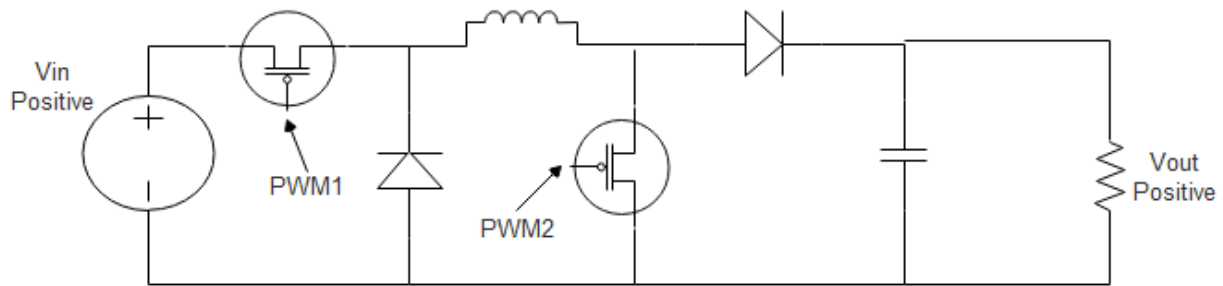


Figure 1.5: Circuit diagram of Non-Inverting buck-boost converter (Switched Mode Power Supplies, p 10)

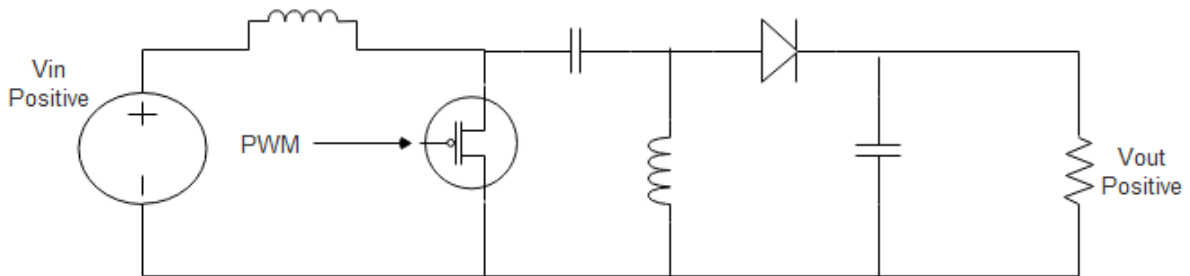


Figure 1.6: Circuit diagram of SEPIC (Keeping. S, 2014)

There are a few algorithms in finding the maximum power point. The most common ones are Perturb and Observe (P&O), Incremental Conductance (InC), Fractional Open-Circuit Voltage(FOCV) and Fractional Short-Circuit Current (FSCC). P&O and InC are both online methods whereas FOCV and FSCC are offline methods. Online methods has the advantage of finding the true maximum power point (MPP) however, there may be power loss due to the oscillations in finding the MPP and also oscillations when it has already reached MPP (Sher.H et. al,2015). Convergence speed is the measure of how quickly the algorithm is able to find the MPP when there is a sudden change in the input source.

*Table 1.7: Table showing the properties of online and offline methods in finding MPP modified from (Sher.HA et. al, p 1426, 2015)*

<b>Online Method</b>	<b>Offline method</b>
Able to track true MPP	Has high convergence speed
Convergence speed depends on step size of algorithm	Needs to isolate from PV when measuring operating point
The faster the speed, the higher the oscillation	Easy to implement

## 1.2 PROJECT OBJECTIVE

Objectives:

1. Design a basic DC-DC converter for renewable energy harvesting.
2. Implement MPPT algorithm for harvesting maximum power in the DC-DC converter.
3. Conduct performance analysis on the designed DC-DC converter.

## 1.3 PROJECT SCOPE

At the end of project 1, a DC-DC converter will be build and the microcontroller MSP432 will be used together with the DC-DC converter. The input voltage and current will be measured and the output voltage and current before going to the battery will be measured. The power loss in between will be computed to find the efficiency of the system. As for comparing this project with the projects mentioned at literature review, this project focuses on the efficiency where efficiency is the priority. As for project 2, in the end, an analysis will be made to compare the efficiency of a buck converter using MPPT and a buck converter without using MPPT and at the same time comparing few MPPT algorithms. This is to study the effects of different ways to improve the efficiency of the charger.

The whole system relies heavily on the renewable energy sources for long term self-sustained operation. If the renewable sources are not able to provide sufficient power to recharge the battery, the system will intelligently go into low powered mode and reduce the drainage of battery.

## **CHAPTER 2: LITERATURE REVIEW**

### **2.0 THEORETICAL AND PRACTICAL STUDY OF A PHOTOVOLTAIC MPPT ALGORITHM APPLIED TO VOLTAGE BATTERY REGULATION**

There are similar projects that have been done in the past. Amara.S et. al (2014) performed a theoretical experiment on building a voltage battery regular. The project models a PV module and creates a boost converter accompanied by a microcontroller that does the MPPT algorithm (Figure 2.1). The project uses MATLAB Simulink as the simulator to get results of the system and comparing it to a direct charging from the PV module to a battery. They used a non-synchronous boost converter and P&O algorithm to find MPP. They achieved positive results in proving that using boost converter and implementing a MPPT algorithm is much more efficient than just to charge directly from PV module to the battery. This is because the fluctuating voltage of the PV module and the battery cannot completely obtain the energy as the input specification of the battery was not followed. However, this system has low efficiency even though it has better efficiency than the stated charging. The boost converter used is the common boost converter that has power losses at components such as diode, transistor, inductor, etc. The MPPT algorithm proposed also has many downsides such as huge oscillations all the time when tracking the MPP. This is a typical problem P&O algorithm has where power are loss during these oscillations.

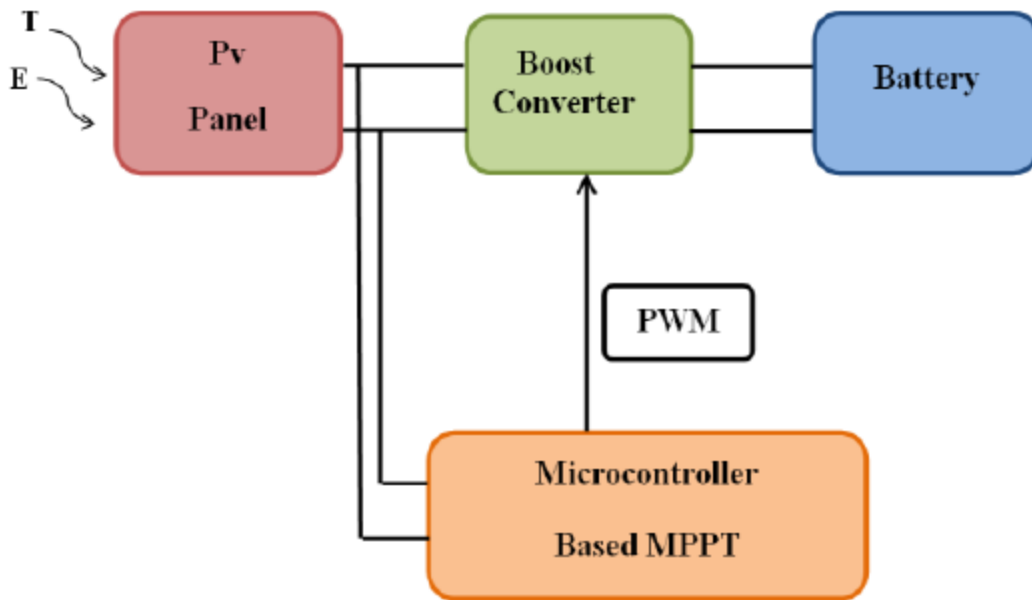


Figure 2.1: The block diagram of the voltage charge regulator (Theoretical and Practical Study of a Photovoltaic MPPT Algorithm Applied to Voltage Battery Regulation, 2014, p. 84)

## 2.1 A NEW SENSORLESS HYBRID MPPT ALGORITHM BASED ON FRACTIONAL SHORT-CIRCUIT CURRENT MEASUREMENT AND P&O MPPT

Sher.HA et. al (2015) proposed a hybrid MPPT algorithm solution that combines the algorithm of P&O (Figure 2.2) and FSSC (Figure 2.3). Using these 2 methods, both advantages of the methods can be combined. P&O has the ability to track the real MPP and FSSC has fast convergence speed. Basically, the system uses FSSC measurement to quickly switch near the real MPP value then P&O will track the true MPP. The strong point of this system has an intelligent mechanism that decides when it is needed to find a new MPP. The mechanism receives PV module current and calculates a value to see if it exceeds a limit which is the sensitivity of the system. Even if there is sudden change of environment conditions, the MPP computed would not suddenly fluctuate. If it exceeds the limit, the short circuit current needed to

calculate the approximate value of MP will be updated. However, this system is difficult to implement as it is very complex. The cost will also be high as more components are needed for the combination of 2 algorithms.

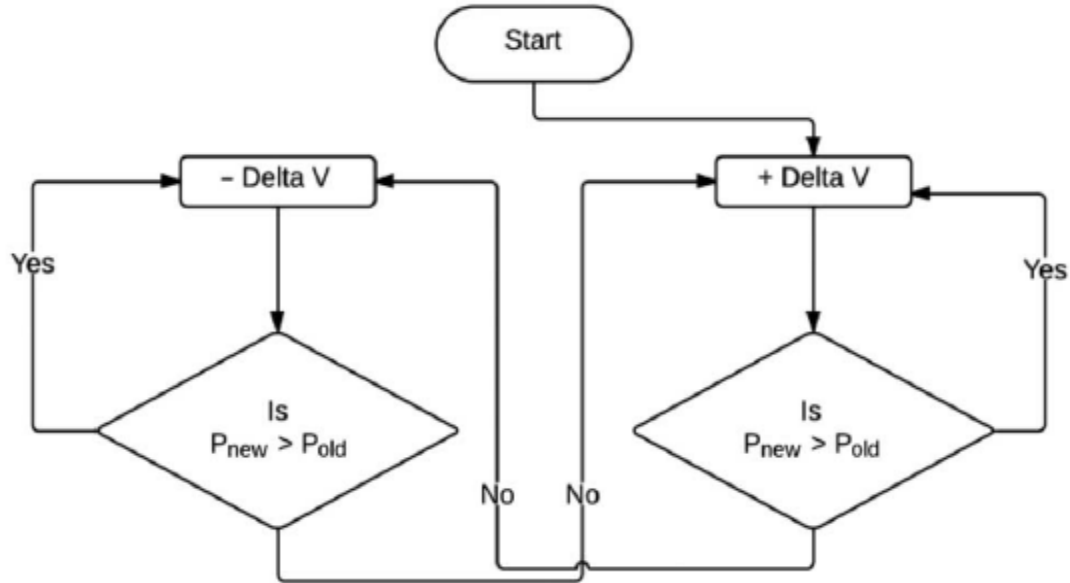


Figure 2.2: Flowchart of the P&O part of hybrid MPPT(A New Sensorless Hybrid MPPT Algorithm Based on Fractional Short-Circuit Current Measurement and P&O MPPT, 2015, p. 1428)

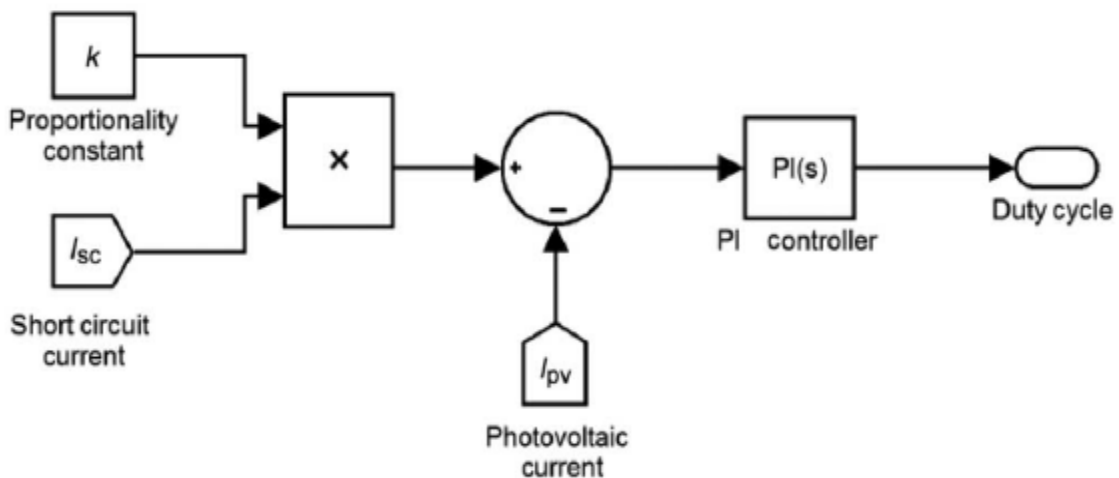


Figure 2.3: Block diagram of the FSCC part of hybrid MPPT(A New Sensorless Hybrid MPPT Algorithm Based on Fractional Short-Circuit Current Measurement and P&O MPPT, 2015, p. 1427)

## 2.2 A FAST PV POWER TRACKING CONTROL ALGORITHM WITH REDUCED POWER MODE

Ahmed.A et. al. (2013) proposed a modified MPPT control algorithm. They modeled a PV generation system as the main source to test the algorithm. A boost converter is used to power a grid converter and a MPPT controller is created to track the MPP (Figure 2.4). The algorithm used is a variable step InC algorithm where instead of using a fixed step to increase or decrease the duty cycle which causes more oscillations, a variable step is used where when the operating point is far from MPP, the step is larger to increase the convergence speed and when it is near the MPP, the step is small to find the exact point of MPP. This algorithm tracks the maximum power point with accurate and fast response, even under the fast changing conditions of solar radiation and temperature. However, the use of this algorithm requires a high frequency processor as every time the operating point is checked, the algorithm computes the step size again no matter how close or far is the operating point from the MPP. Therefore, a costly microcontroller would be needed to accommodate the high frequency criteria.

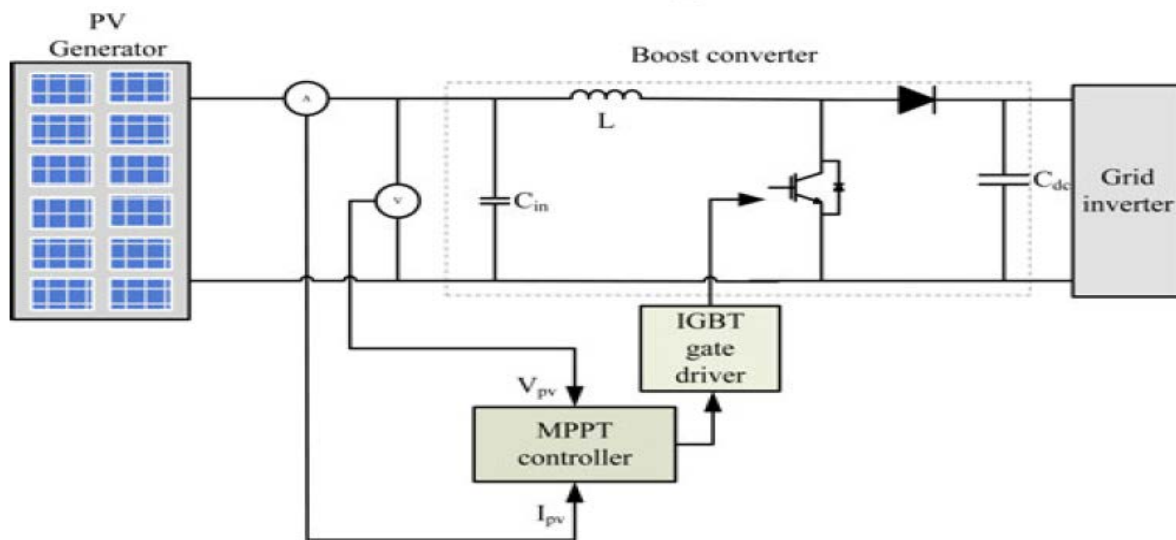


Figure 2.4: Block diagram of the overall system (A Fast PV Power Tracking Control Algorithm With Reduced Power Mode, 2013, p 566)



## CHAPTER 3: SYSTEM DESIGN

### 3.0 PROPOSED BUCK CONVERTER

This buck converter is capable of maximizing the efficiency from the input source which will be a renewable energy source to a battery. The buck converter would be of the synchronous buck converter that is a little different than the generic buck converter. Referring to Figure 3.1 instead of using a diode, another MOSFET is used to replace the diode. This is because diodes have higher forward voltage drop and losses more power compared to the switching loss in MOSFET. This is to further increase the efficiency of the converter. M1 and M2 must not activate at the same time as it will result in short circuit. M2 must act like the diode that has been replaced. When M1 is on, M2 will be off to allow current to flow to L1. When M1 is off, M2 must allow current to flow from C1 or L1 back to L1 to achieve complete circuit.

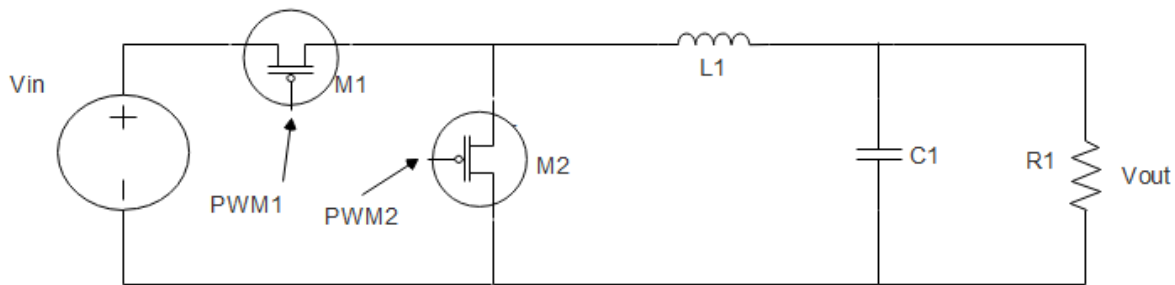


Figure 3.1: The circuit diagram for a synchronous buck converter

The MOSFET chosen is the IRFZ44N which is an N-channel MOSFET in high side that needs to be driven by a MOSFET driver, IR2104. Based on the datasheet, IRFZ44N has a  $R_{ds(on)}$  of 17.5 m ohm. Which means when the MOSFET turns on, it will have a resistance of 17.5 m ohm from drain to source where the lesser the better because high resistance results in higher voltage drop, which leads to more power loss and reduces efficiency.

The voltage in the microcontroller is insufficient to turn on the MOSFET.  $V_{gs}$  is the voltage required to turn on the MOSFET and this parameter value can be calculated. The

minimum value of  $V_{gs}$  must be more than  $V_{th}$ , which is the threshold voltage. How much increase depends on the load resistance on the source of the MOSFET.  $V_s$  is the voltage at the source of the MOSFET.

$$V_{gs} > V_{th}$$

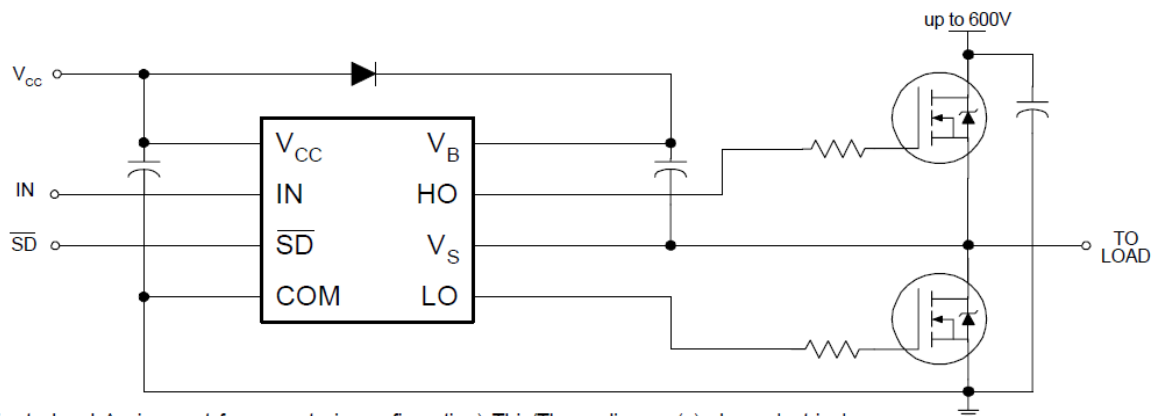
$$V_g - V_s > V_{th}$$

$$V_g > V_{th} + V_s$$

This inequality is only applicable for high side switching where the load is at the source of the MOSFET and the drain is supplied by  $V_{cc}$ . Since the input voltage will be around 12V, the source voltage will be a little lesser than the input voltage depending on the load resistance and  $R_{ds(on)}$  of the MOSFET.

$V_{gs}$	Gate to source voltage, voltage required to turn on.
$V_g$	Gate voltage, voltage supplied to the gate
$V_s$	Voltage at the source of the MOSFET, depends on the impedance of load
$V_{th}$	Threshold voltage, minimum voltage needed to turn on the MOSFET if the source is grounded.

The typical connection of the IR2104 are as follows:



(Refer to Lead Assignment for correct pin configuration) This/These diagram(s) show electrical connections only. Please refer to our Application Notes and DesignTips for proper circuit board layout.

Figure 3.2: Typical connection of the IR2104 (Data Sheet No. PD60046-S)

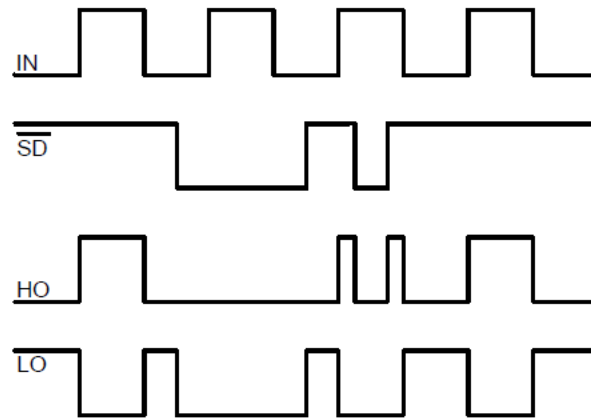


*Figure 3.3: Function diagram of the IR2104 (Data Sheet No. PD60046-S)*

When  $\overline{SD}$  is high, HO has the exact waveform of IN but with higher voltage. The voltage depends on the voltage pumped in the Vcc. LO is the exact inverse of HO when  $\overline{SD}$  is high. Therefore, HO can be used to drive 1 MOSFET and LO can be used to drive another MOSFET in the synchronous buck converter.

The MPPT algorithm used would be Incremental Conductance which would not be too complex. This algorithm has better efficiency compared to P&O. Mouybyed.N (p 778, 2009) pointed out that incremental conductance can determine precisely when the MPP is reached and it does not oscillate about when MPP is reached.

### 3.1 SIMULATION OF BUCK CONVERTER

Simulation for the buck converter is has been done in Multisim 13.0. The input voltage for this simulation is 12V because most PV panels are rated in 12V and the desired output voltage is 5V. Actual components are used just to watch the concept of buck converter to study the power losses in the components. The duty cycle is set at 41.6% and is passed by a square wave source that will ideally get 5V. Hence, the output has a stable 5V with 0.1V tolerance. In real circuit, a NOT gate is not used but a gate driver, IR2104 can increase the voltage of PWM to turn on the MOSFET and has an internal inverter that inverts the output.

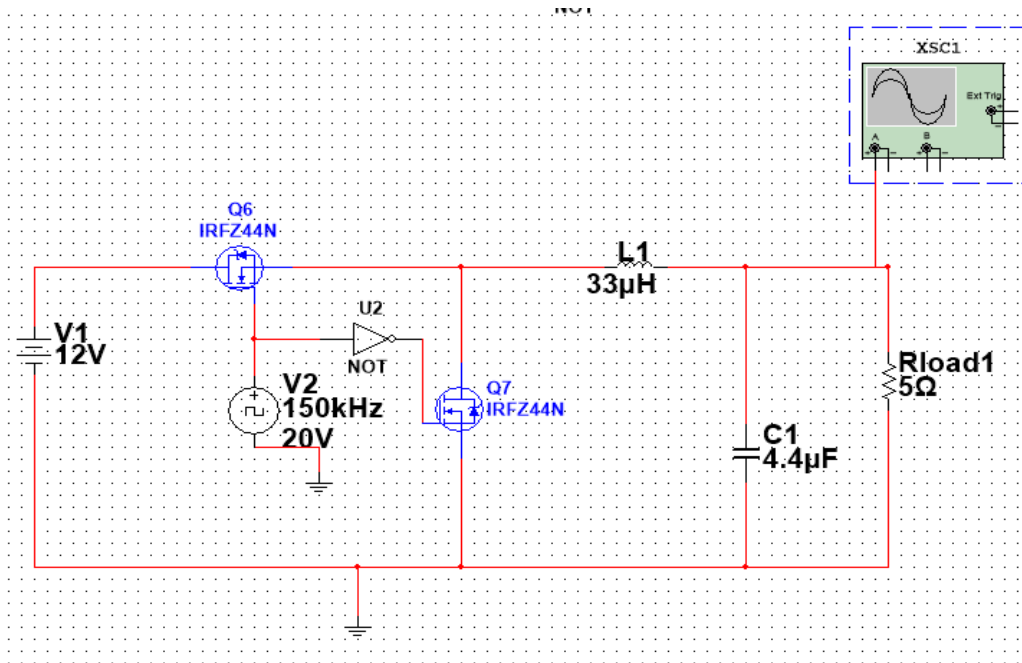


Figure 3.4: The simulation circuit for buck converter

For the values calculation,  $L = (V_{in} - V_{out}) \times \frac{\text{Duty Cycle}}{\text{Switching frequency}} \div \text{Ripple current}$

Let ripple current be around 0.9 A.

$V_{in}=18\text{V}; \quad V_{out}=7.2\text{V}; \quad \text{Duty cycle}=5/12=40\%; \quad \text{Switching frequency}=50\text{KHz}$

Therefore, the inductor value is 94.8  $\mu$ H. There is no exact 94.8  $\mu$ H inductor in the market and therefore it is rounded up to 100  $\mu$ H.

One of the important parameter for the capacitor for a DC-DC converter is the output ripple voltage. That is the main concern for the capacitor. The ripple can be observed at output voltage in the oscilloscope in Figure 4.9. The capacitor size affects the ripple output voltage. The higher the size, the more the ripple but the voltage is more stable after some time based on the simulation made. Therefore, a suitable size must be chosen. To optimize the output filter performance it is recommended to target 20% – 40% inductor ripple current, which translates to a current ripple ratio of 0.18 – 0.36 (LC Selection Guide for the DC-DC Synchronous Buck Converter, p 3, 2013). Let current ripple ratio be 0.27.

$$C = \frac{\Delta L}{8 \times \text{Switching frequency} \times \Delta V_r}$$

$\Delta V_r$  = Output ripple voltage peak to peak = 0.05V

$\Delta L$  = Output Current = Current Ripple ratio  $\times$  ( $V_{out}/R_{out}$ ) = 0.27 $\times$ ( $V_{out}/R_{out}$ ) = 0.45 A

C = capacitance of capacitor

Switching frequency = 50 KHz

The C value calculated is 22.5  $\mu$ F and therefore it is rounded down to 22  $\mu$ F.

The switching frequency is inversely proportional to the size of the inductor and capacitor and directly proportional to the switching losses in MOSFETs (Back to Basics: The Importance of Switching Frequency, 2013). The higher the switching frequency of MOSFET, the lower the size of the inductor and capacitor which are cheaper but the higher the switching loss of MOSFET. However, lower switching frequency also causes conduction losses in the MOSFET (Cooper. C, 2013). Therefore, a switching frequency of not too high or too low is chosen which is 50 kHz.

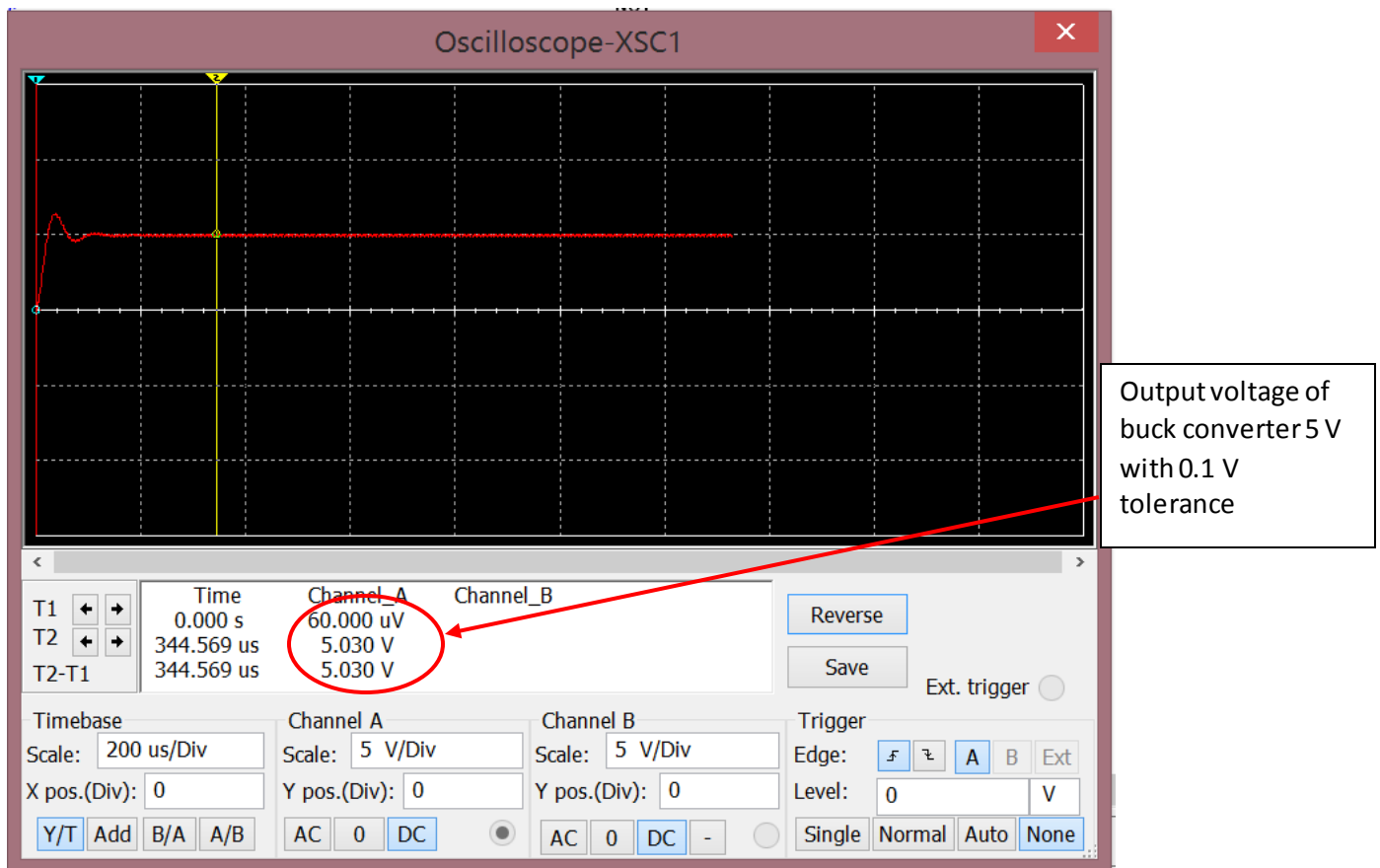


Figure 3.5: The simulation result for the buck converter

### Calculation of Efficiency

Since the input current cannot be obtained because the source is a voltage source, power cannot be calculated and compared within the input power and output power. Hence, voltage will be used to find the efficiency. Using theoretical voltage based on the duty cycle ratio and the output voltage obtained from oscilloscope.

$$V_o = \frac{41.7}{100} \times 12$$

$$V_o = 5V$$

From oscilloscope,  $V_o = 4.71V$  to  $4.99V$ . Average =  $4.85V$

$$Efficiency = \frac{4.85}{5} \times 100\%$$

$$Efficiency = 97\%$$

However, these are only from simulations. In practical, there are more losses that Multisim neglects such as power losses in wires and protoboard.

### 3.2 SELECTION OF MICROCONTROLLER

Microcontroller plays an important role in this system as the switching frequency of the buck converter is supplied by the microcontroller. Therefore, the microcontroller must be able to supply the needed frequency. Besides, the microcontroller must have feature like PWM (Pulse Width Modulation) to be able to change the duty cycle for the buck converter. Another feature that is essential is ADC (Analog to Digital Converter). ADC is needed to obtain the input from the renewable energy and to be converted digitally to process the value. In this case, it is processed in the microcontroller based on the MPPT algorithm to output the respective duty cycle.

There are a few choices available but the selections are limited to the price and features since efficiency and cost is the priority. Microcontroller must be able to have at least 2 channels of PWM, 2 ADC channel, low powered and able to generate 50 kHz PWM frequency at the lowest cost possible. Based on these criteria, the microcontroller that is suitable is MSP432P401R from Texas Instrument. However, due to lower tolerance of voltage in the pin of MSP432, the pin that is supposed to provide pulse wave keeps getting damaged because of the 5V output from the gate driver when there is no input from the Vcc. The 5V comes from the SD pin which is supplied by the microcontroller. The maximum voltage for the pin to accept is 4.17V and hence, this microcontroller is unusable for this system unless another gate driver is used.

Arduino Uno is used in replace of the MSP432. Arduino has higher voltage pin tolerance;  $V_{cc}+0.5\text{ V}$  (5.5V). Arduino Uno also have the required resources for this system. For example, a 12bit timer for PWM, 4-channels of ADC and serial port or I2C to display voltage, current, power, efficiency and state of the system. However, there is a downside in using this microcontroller. This microcontroller has the resolution of 10-bit for ADC, which means that with the current sensor that is selected, every step (total of  $2^{10}=1024$ ) has the current detection accuracy of 0.026A/step. The current sensor used, ACS712-5A has the best accuracy compared to the 10A and 30A versions as the 5V of  $V_{cc}$  is used to measure the range of only -5A to 5A. This gives the best accuracy and resolution for the 10-bit ADC.

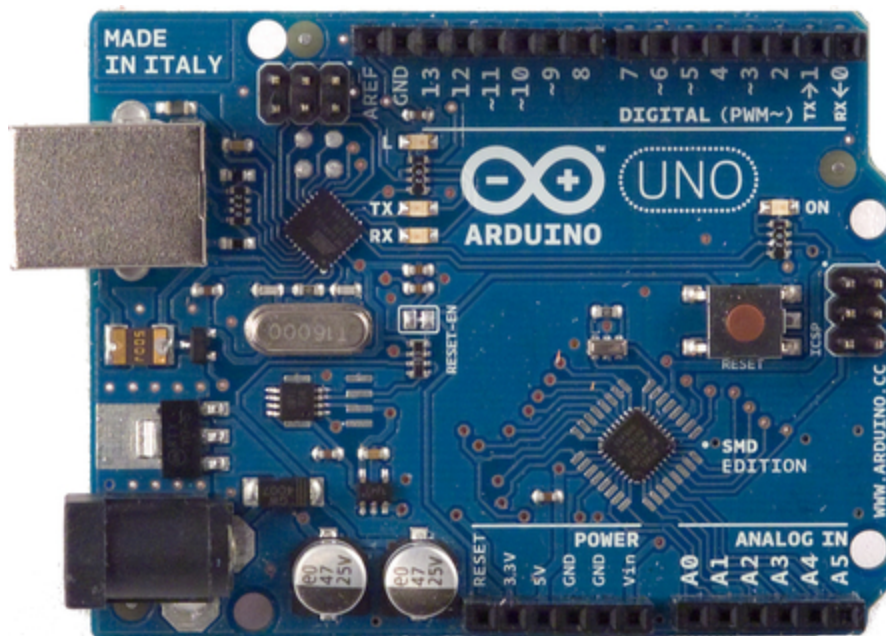


*Figure 3.6: Board view of the Arduino Uno*



### Microcontroller Specification

- 16MHz
- 8-bit ATmega328
- 32KB Flash
- 2KB RAM
- 6ch 10-bit ADC
- 1 12-bit, and 2 8-bit Timers
- I2C, UART

The microcontroller will be used to track the MPP. This is a microcontroller based on ATmega328 processor that is suitable specifically for low cost and embedded applications. It is priced at RM32.90 as listed in [lelong.com](http://lelong.com).

The microcontroller will be used to compute the duty cycle using InC algorithm and at the same time calculate the power efficiency. Figure 3.6 shows a feedback to the microcontroller at the cathode of the load. By this way, the efficiency can be calculated by comparing  $V_{in}$ ,  $C_{in}$  and  $V_{out}$ ,  $C_{out}$  and displaying the  $V_{in}$ ,  $V_{out}$  and efficiency using an LCD screen (RGB backlight LCD by Grove). With the input voltage and current, the power can be calculated. Using the equation below, the efficiency can be calculated.

$$Efficiency = \frac{V_{out} \times C_{out}}{V_{in} \times C_{in}} \times 100\%$$

Arduino 1.6.5 would be used to code, program and flash codes into the microcontroller. The microcontroller is powered via battery and windows PC (Personal Computer) to code and program into the microcontroller. The language used will be an arduino based structure polling with C language functions.

### 3.3 HARDWARE AND COMPONENTS REQUIRED

#### IR2104

This is the gate driver to drive the gate of 2 MOSFETS for high side and low side switching.

#### IRFZ44N

This is an N-channel MOSFET used to alternately switch in between to allow on and off time of the buck converter

#### Arduino Uno

This is the microcontroller used to measure current and voltages, compute efficiency and power, run the MPPT algorithm and provide PWM pulse accordingly.

#### 100uH toroidal inductor

This is the inductor used to store current during on time and discharge current during the off time.

#### 22 uF capacitor

This is the capacitor used to reduce ripple of the buck converter output voltage.

#### 100k, 20k ohm resistors

This are the resistors used to create a voltage divider to scale down the input voltage to a smaller voltage for the microcontroller to detect.

#### ACS712 hall-effect based current sensor

This is the current sensor used to detect current for both input and output current. The benefit of this sensor is that it isolates the detection circuit and the main circuit to prevent any power loss of the main circuit.

#### Grove-RGB backlight LCD 16x2

This is the LCD used to display the input and output voltage, input and output current, the state of the charger and efficiency.

#### NTE519

This is the diode used to prevent current flow back to the buck converter and the solar panel when the solar panel is not producing power.

#### 15W solar panel

15W polycrystalline solar panel is used as the main power source for the buck converter to charge a battery.

#### 7.2V 2000mAh Ni-Cd battery

This nickel cadmium battery will be used to charge as this type battery will not explode. However, the trade-off will be high self-discharge and has memory effect. Memory effect is the effect on batteries where the battery tends to remember its smaller and smaller capacity after many charge cycles. This can be fixed with a full discharge and a full charge.

### 3.4 CIRCUIT SETUP

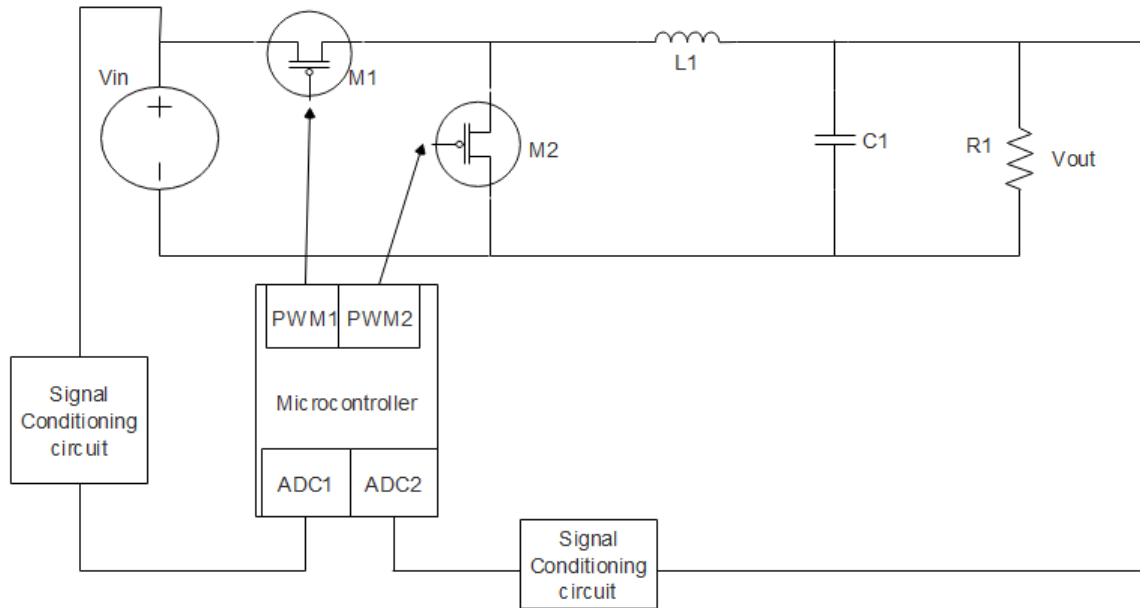


*Figure 3.7: Circuit diagram of the Synchronous buck converter with microcontroller as the controller to find MPP*

ADC in the microcontroller is needed to measure the input voltage, current and output voltage, current. However, there are limitation in the microcontroller. The arduino pin can only accept voltage levels of maximum 5.5 V based on the datasheet and any higher voltage will permanently damage the pin of the microcontroller. Therefore, voltage divider circuit is used to reduce the voltage to the voltages supported by the microcontroller. Then, software is used to calculate the actual voltage based on the voltage divider resistance ratio.

Some calibrations need to be made to the voltage divider. Since the internal reference of the ADC is 5V and the ratio of 1:6 is used. This can be done using 100k ohm and 20k ohm resistors. This means that if 6V is supplied, the microcontroller will read the value of 1V and using coding, 6V will be computed back in digital.

As for current measurement, ACS712 hall-effect current sensor is used. The Vcc pin is supplied by the microcontroller and the IP pin is used to detect the current. The Vout will give out respective voltage based on the current. To retrieve the voltage, this formula is used.

$$\text{Current} = \frac{\text{ADC voltage} - 2.5}{0.185}$$

The equation above is derived from ACS712 datasheet. As there will be 2.5V in output even when there is no current, the voltage detected needs to subtract by 2.5. 0.185 V/A is the gradient for the graph of Vout over input current.

However in practical, the supply voltage to the microcontroller is not exactly 5V. This leads to inaccuracy in the current measurement formula. Due to incorrect display in ADC value, sensor's error from frequent usage and the real current measurement error, new calibration needs to be made for each current sensor.

Firstly, the voltage from ADC microcontroller is measured when no current is supplied, usually around 2.48-2.5V. Then, measure the voltage from the current sensor's Vout when current is supplied. Use the formula above to derive the gradient for the current sensor where its default is 0.185. After that, verify its correctness with different current values supplied. For example,

$$0.19A = \frac{2.5 - 2.485}{x}$$

$$x = 0.028180$$

### 3.5 MICROCONTROLLER CODING SETUP

#### PWM setup

The library TimerOne is used and the pin9 with 12-bit timer1 is used for PWM. For frequency, it is  $1/20\mu\text{s} = 50\text{KHz}$ .

```
Timer1.initialize(20);    // initialize timer1, and set a 20uS period 50kHz
Timer1.pwm(PWM_PIN, 0);   // setup pwm on pin 9, 0% duty cycle
Timer1.pwm(PWM_PIN, (PWM_FULL - 1), 20); //PWM_FULL=100 this is to change the
duty cycle of the pulse wave eg. 99%
```

#### ADC setup

The setup below configures 2 channels for voltage reading and 2 channels for current reading. Another function is used to compute the average of 8 readings for a more stable reading.

```
#define SOL_AMPS_SCALE 0.053662055 // the scaling value for raw adc reading to get
solar amps 5/(1024*0.185)
#define SOL_VOLTS_SCALE 0.029143228 //the scaling value for raw adc reading to get
solar volts (5/1024)*(R1+R2)/R2 R1=100k and R2=20k
#define BAT_VOLTS_SCALE 0.029143228
#define AVG_NUM 8

int compute_avg(int channel){
    int sum = 0;
    int temp;
    int i;

    for (i=0; i<AVG_NUM; i++) {
        temp = analogRead(channel);    // read the input pin
        sum += temp;                  // store sum for averaging
        delayMicroseconds(50);        // pauses for 50 microseconds
    }
    return(sum / AVG_NUM);           // divide sum by AVG_NUM to get average and return it
}
```

```
void read_data(void) {  
  
    sol_amps = (compute_avg(SOL_AMPS_CHAN) * SOL_AMPS_SCALE -27.323);  
    if(sol_amps < 0)  
        sol_amps = 0;  
    sol_volts = compute_avg(SOL_VOLTS_CHAN) * SOL_VOLTS_SCALE;  
    bat_volts = compute_avg(BAT_VOLTS_CHAN) * BAT_VOLTS_SCALE;  
    sol_watts = sol_amps * sol_volts ;  
}
```

### State of Charge setup

This state of charge is to show the capacity left on the battery using voltage. If the capacity is near empty, its voltage would be around 5.96V; just before the microcontroller would not work properly. At its full charge capacity, the voltage of the battery is around 7.82V as measured when the voltage would not rise anymore despite the power is still connected.

```
pct = 100.0*(bat_volts - 5.96)/(7.82 - 5.96);  
if (pct < 0)  
    pct = 0;  
else if (pct > 100)  
    pct = 100;
```

## **LIBRARIES USED**

### TimerOne

This library is used to set the pwm frequency at 50Khz and modifying the duty cycle using Timer1.pwm() function. This library used timer1 which is 16bit.

### Rgb\_lcd

This is the display library for Grove- Backlight LCD that can change the color of backlight, setting cursor to display digits or characters. This can only be used in 16x2 dimension. This library uses I2C to communicate with the microcontroller. This communication is used because of the less pins needed between the LCD and the arduino. Only 2 pins are needed, SCA and SCL pins.

### Sleep

This library is used to put the microcontroller into sleep. The mode of POWER\_DOWN sleep mode will be used as it is the most power saving mode. Many configurations are needed because during sleep, most functions and peripherals will be disabled. Before sleep, the ADC register must be saved, the interrupt for waking up must be configured and the sleep mode must be set. After waking up, the ADC registers must be restored, sleep must be disabled, interrupt must be detached and I2C for the LCD must be reconfigured. The only peripheral that does not need configuration before and after sleep is timer.



### **3.6 PINS AND PORTS USED IN MICROCONTROLLER**

A0 - Voltage divider (solar)

A1 - ACS 712 Out (solar)

A2 - Voltage divider (battery)

A3- ACS 712 Out (battery)

A4 - LCD SDA

A5 - LCD SCL

D2 - Push-button

D8 - 2104 MOSFET driver SD

D9 - 2104 MOSFET driver IN

GND – Battery GND, LCD GND, Voltage divider GND, ACS712 GND, MOSFET gnd

5V – ACS 712 Vcc, LCD Vcc, push-button reference

RX – RX of the wireless serial transceiver module

TX – TX of the wireless serial transceiver module

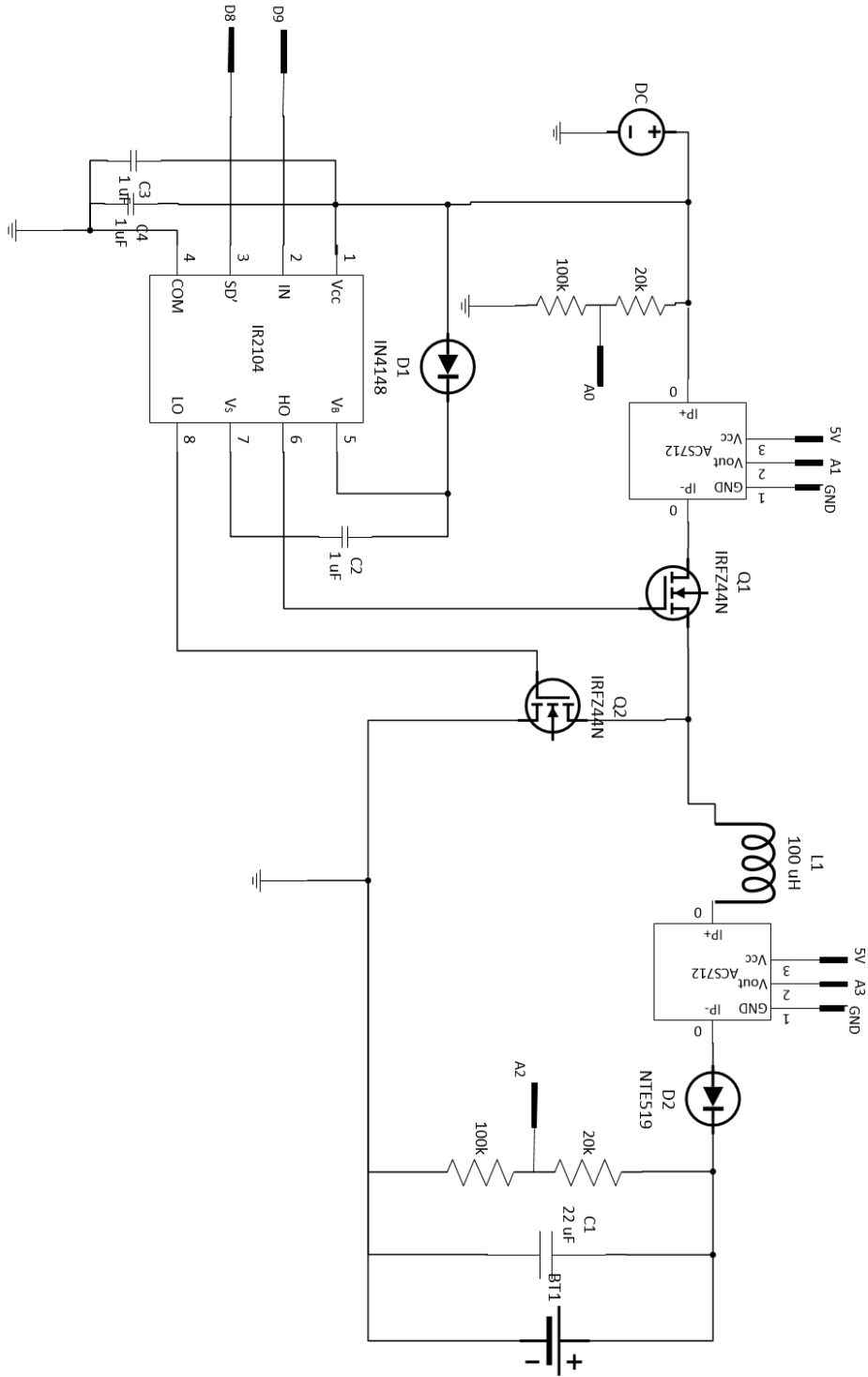


Figure 3.8: Circuit schematic of the Synchronous buck converter

### 3.7 FEATURES OF THE CHARGER

This charger is capable of changing its state of charge depending on the solar power itself and the battery voltage supplied. There are 4 states implemented on the charger; ON, OFF, BULK and FLOAT. Additional details are explained in the next sub-chapter.

This charger can be used to power an IoT device or act as an IoT device itself by logging data through wireless UART to devices like PC or any device that supports UART and has a USB connector. The devices used is the UC00B, UART to USB converter and the wireless serial transceiver module. One transceiver module to transmit data from the microcontroller and one to receive the data and pass to the UART to USB converter to the PC. Data such as voltage, current, power, efficiency etc can be read through the device in a serial monitor wirelessly.

Besides, any rechargeable battery can be used to charge as long as the rated input voltage of the battery is below the voltage of the solar panel. Some modifications need to be done on the codes of the microcontroller. The charger is also capable of turning itself to sleep if there is no input in the solar panel after 5 seconds. This is to save electricity and reduce the draining of the battery to power the microcontroller if no power source is detected.

The charger also has reverse flow protection that prevents backflow of current back to the buck converter and the solar panel when the solar panel is not producing power. A diode, NTE519 with the max voltage drop of 1V is used. This diode is used because this diode is for high speed switching and it is suitable to be used for the buck converter's 50 kHz switching frequency.

This system only needs 1W of power from the solar panel to charge the battery as the microcontroller itself consumes around 0.7W with the LCD on. If the LCD is disconnected, the system only needs around 0.6W of power to sustain itself.

### 3.8 OPERATION STATES OF THE CHARGER

The states of the charger is required to create a more intelligent charger. The role of the states is basically to prevent damage to battery, improve efficiency of the charger and maximize available power of the solar panel to the battery. However, there are states that are not stable as the solar panel requires load in the buck converter to supply current to the converter and in order to do that, the state of the charger must first be ON in order to activate the gate driver and turn on the MOSFETS. To fix this problem, the state ON is switched to when the voltage of the solar panel exceeds 4.5V.

The float state is to prevent overvoltage to the battery. This state turns off the MOSFET if the battery voltage exceeds 8V and try to maintain the battery voltage at 7.8V. If the voltage drops lower, it changes into the bulk state.

The bulk state is the most crucial state of the charger. This is the state where the MPPT algorithm Incremental Conductance is placed. The requirement to enter this state is that the solar panel must provide at least 2W and the duty cycle will be adjusted accordingly to yield the maximum power.

*Table 3.9: Different states' condition and description*

State	Condition	Description
Off	Activates on startup and when solar voltage < 4.5V and solar power < 1W	This is to prevent charging the battery when the power is too low from the solar panel. Charging below 4.5V does not charge the battery.
On	Activates when $1W < \text{solar power} < 2W$ or solar voltage > 4.5V	This is pass the full power of solar panel to the battery with max duty cycle (99%).
Bulk	Activates when solar power > 2W and solar voltage > 4.5V	This is to charge the battery normally and use MPPT algorithm

		to track the MPP until the battery voltage reaches 5.2V
Float	Activates when battery voltage > 8.0V	This is when the battery voltage exceeds 8.0V and this float state reduces the voltage by turning of the MOSFETS.

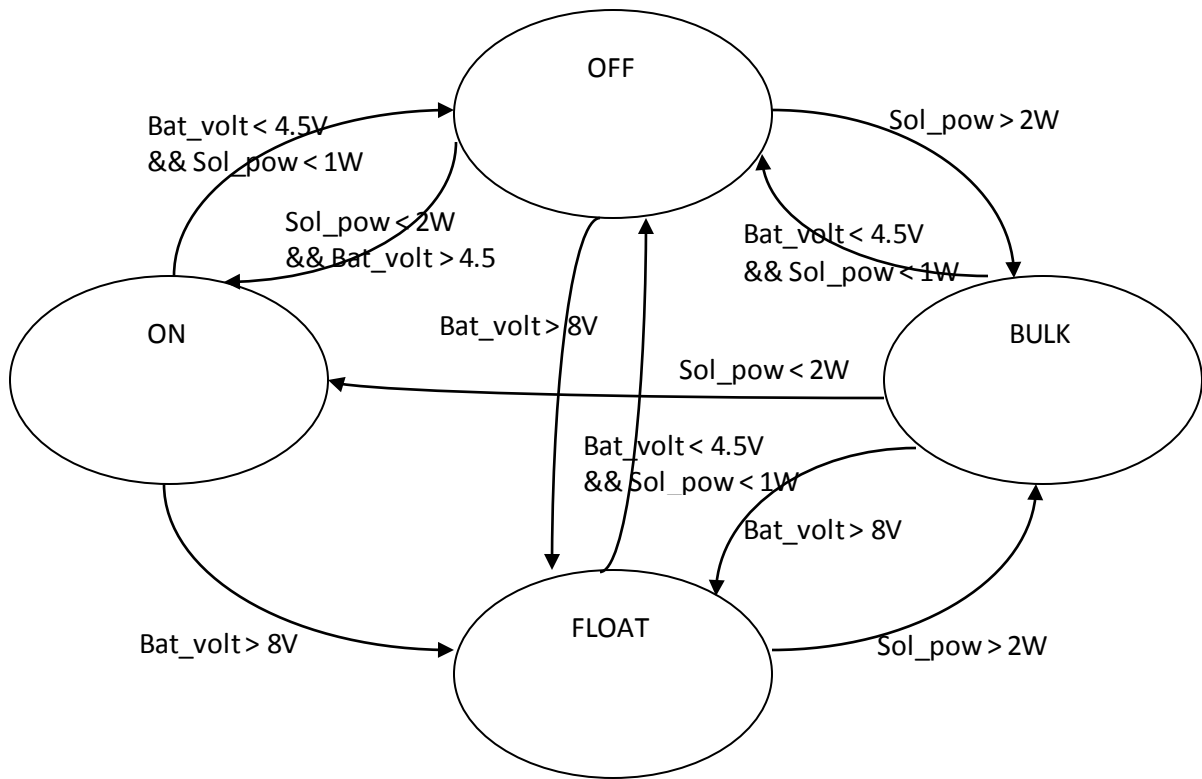


Figure 3.10: The operation state diagram of the system

### 3.9 AUTO-SLEEP FEATURE

This feature helps the system in saving more power by cutting off power to the microcontroller when the solar panel is disconnected or not producing power. To implement this feature, additional circuit to activate the microcontroller is needed. A push-button is also needed to activate the microcontroller by close-circuiting the power to the microcontroller when the button is pressed. Therefore, the activation of the microcontroller is controlled by either the push-button or the digital pin in the microcontroller.

When the solar voltage is 0V or disconnected for 5 seconds, sleep will be activated. If there is voltage within this 5 seconds, the timer will be stopped and reset. This sleep mode is of the `POWER_DOWN` obtained from `sleep.h` library. This sleep mode reduces the most power consumption; only activating `INT0` (D2 pin) and `INT1` (D3 pin) external interrupt, `TWI Address Match` and `WDT` (Watch Dog Timer). The other clock domains like `CLK` (CPU), `CLK` (FLASH), `CLK` (I/O), `CLK` (ADC), `CLK` (ASY); oscillators like main clock source, timer oscillator and wake-up sources like `timer2`, `EEPROM`, `ADC` and other I/O will be disabled.

During sleep, the Arduino consumes 20mA which is considerably low. If the power LED on board could be turned off, the power consumption would be even lower. However, there is no such way to do it using software as the power to the microcontroller is directly connected to the LED.

### 3.10 SPECIFICATION OF SOLAR PANEL

The solar panel used are the WN-15 which is capable of providing maximum of 15W of power under load. This solar panel uses polycrystalline silicon solar cells which has lower heat tolerance and lesser efficiency as compared to mono-crystalline silicon solar cells.

*Table 3.11: The solar panel's specification and characteristics*

Characteristic	Value
Maximum Power	15W
Open-circuit Voltage	21.5V
Short-circuit Current	0.98A
Maximum Power Voltage	17.5V
Maximum Power Current	0.85A



*Figure 3.12: The 15W solar panel used for the system*

### **3.11 CHARGING THE BATTERY**

The process of charging is started when the potential difference is met with the specifications of the battery and when current is supplied to the battery. As for the battery that is used, the input that is accepted is usually higher than 7.2V as 7.2V is the nominal voltage. The max current that is accepted has a wider range of between 0-2A. However, using battery, there will be concerns on reverse electric flow back to the system when the solar panel is not connected. An extra diode has to be placed to prevent back flow of electricity. The state of charge of the battery can be determined using voltages where at the peak capacity the battery supplies 8.0V and at the least capacity is lower than 6.2V. 6.2V is considered at 0% state of charge as that is the minimum voltage for the Arduino Uno to work properly. The Arduino has a built in voltage regulator that has the voltage drop of 1.2V and support voltages of up to 12V.



## CHAPTER 4: METHODS/TECHNOLOGIES INVOLVED

In this project, a buck converter will be build and hence the operation this buck converter will be discussed in detail. PWM is a control used by setting the switch rate for a switch. It is a square wave signal that has control of the duty cycle of the square pulse. Figure 4.1 shows a better look at the concept of PWM in controlling switching. As for how a DC-DC converter operates, the reduction of the voltage is controlled by controlling the duty cycle. For example, an input voltage of 12 V will need a duty cycle of 41.6% to be stepped down to 5V.

$$V_{out} = \text{Duty Cycle} \times V_{in}$$

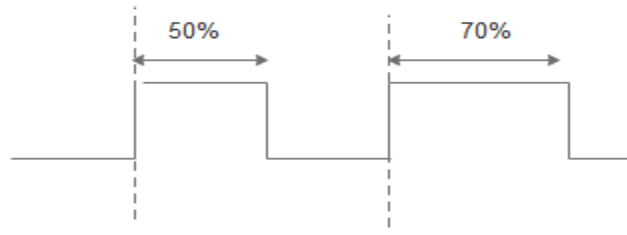


*Figure 4.1: Square wave with the duty cycle of 50% in the first period and duty cycle of 70% in the second period.*

### 4.0 OPERATION OF BUCK CONVERTER

Referring to the circuit in Figure 4.2, when the MOSFET is in the ON period current flows from the source to M1 and to L1. The current does not flow to D1 as the diode is in reversed-bias mode. There will be a huge positive charge at the cathode of D1 resulting no current flow through D1. The charge in L1 builds up gradually and does not allow current to pass to C1 and R1 at the beginning. When the charge stored in L1 is full, R1 receives current and C1 begins charging. Following up, the current does not flow to D1 as the current from source will always prefer ground of the source even though the D1 will be in forward biased from that direction of current.

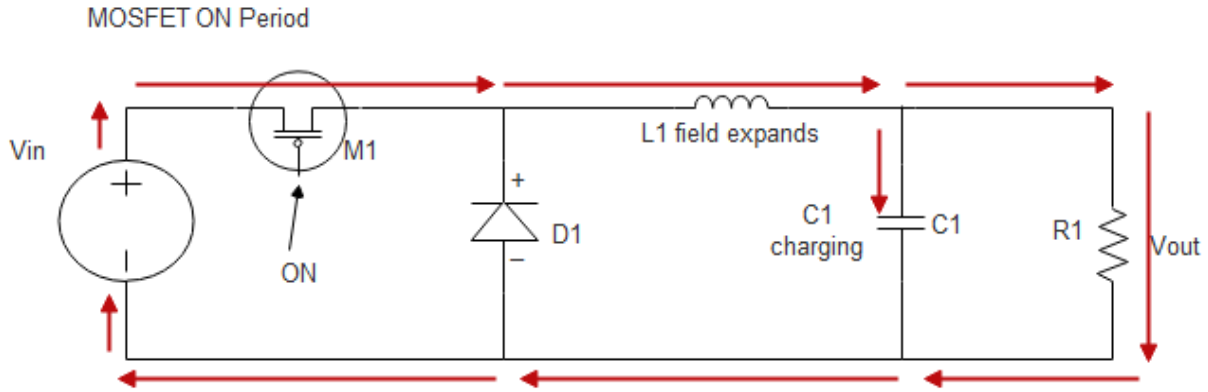


Figure 4.2: Buck converter operation during M1 on period (The red arrow shows the direction of current)

Referring to Figure 4.3, when M1 is in off period, even if the source is still providing current, M1 will not allow current to flow from source to drain on M1 because the gate is turned off. L1 first supplies current as a back e.m.f (electromagnetic field) from the built up charge to R1 where the load is supposed to be. The current will continue to flow to D1 as the diode now acts in forward biased mode. This makes the circuit complete. After the field in L collapses, C1 will replace L1 as the current provider like the flywheel effect. The L1 and C1 provide current until the M1 is turned ON again to recharge L1 and C1.

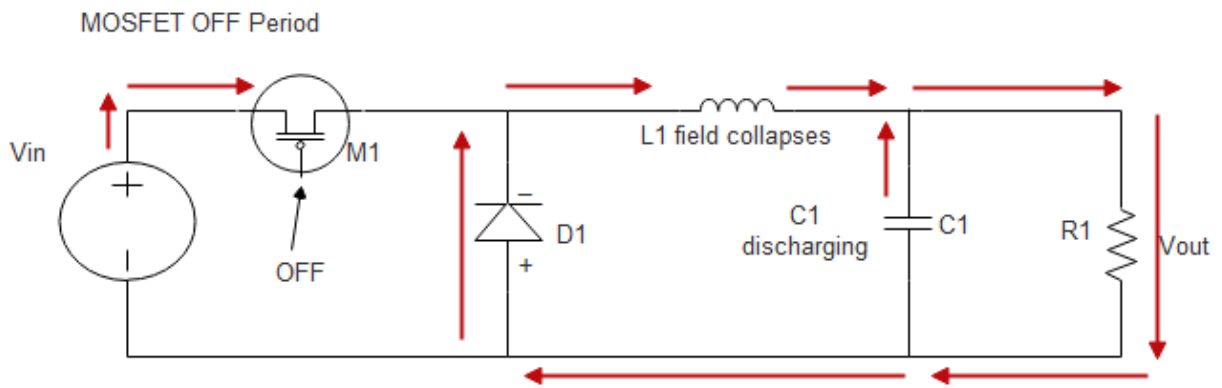


Figure 4.3: Buck converter operation during M1 off period (The red arrow shows the direction of current)

The overall duration of M1 on and off creates a ripple voltage at R1 around the desired voltage. The ratio of the on and off of M1 is controlled by PWM or the duty cycle of square wave as explained above. However, there are more complications when the objective is to obtain a high efficiency power output. As there would be power losses in all components (Nowakowski, R, King. B, 2006). M1 will have power losses in switching, conducting and turn-on voltage at the gate. D1 would have forward voltage drop whenever a current passes. L1 and C1 will also have power losses but the losses are not much if low resistance components are chosen. Therefore, Cooper.C (2013) wrote an article in Fundamentals of Buck Converter Efficiency stating that the choice of MOSFET with low on-resistance and low gate charge will be essential for efficient buck converter. It also mentioned that the power losses for inductor to minimize are core losses and low DC resistance. As for diode, the only parameter is the forward voltage drop and if these parameters could be at minimal, the buck converter would be very efficient.

#### 4.1 OPERATION OF MPPT ALGORITHMS

P&O and InC will be discussed in detail as these 2 algorithms are the most commonly used algorithm for Maximum Power Point Tracking (MPPT) (Comparative Analysis Of The Perturb-And-Observe and Incremental Conductance MPPT Methods, p 60, 2014). P&O also known as the hill climbing method finds the MPP by continuously reading the source voltage and current at a fixed frequency. The concept is to keep comparing the computing the new input power through the input voltage and input current by multiplication and comparing the power with the old power value calculated previously. If the new power is larger than the previous power, there is a new MPP and the control of duty cycle to the buck converter needs adjustment. The difference of voltage is also needed to be computed to indicate the direction of perturbation of the MPP. The adjustments are through increasing or decreasing the duty cycle by the step size. The larger the step size, the faster the convergence speed but it would result in higher oscillations even after reaching MPP. Refer to Figure 4.4 for better understanding on the P&O algorithm.

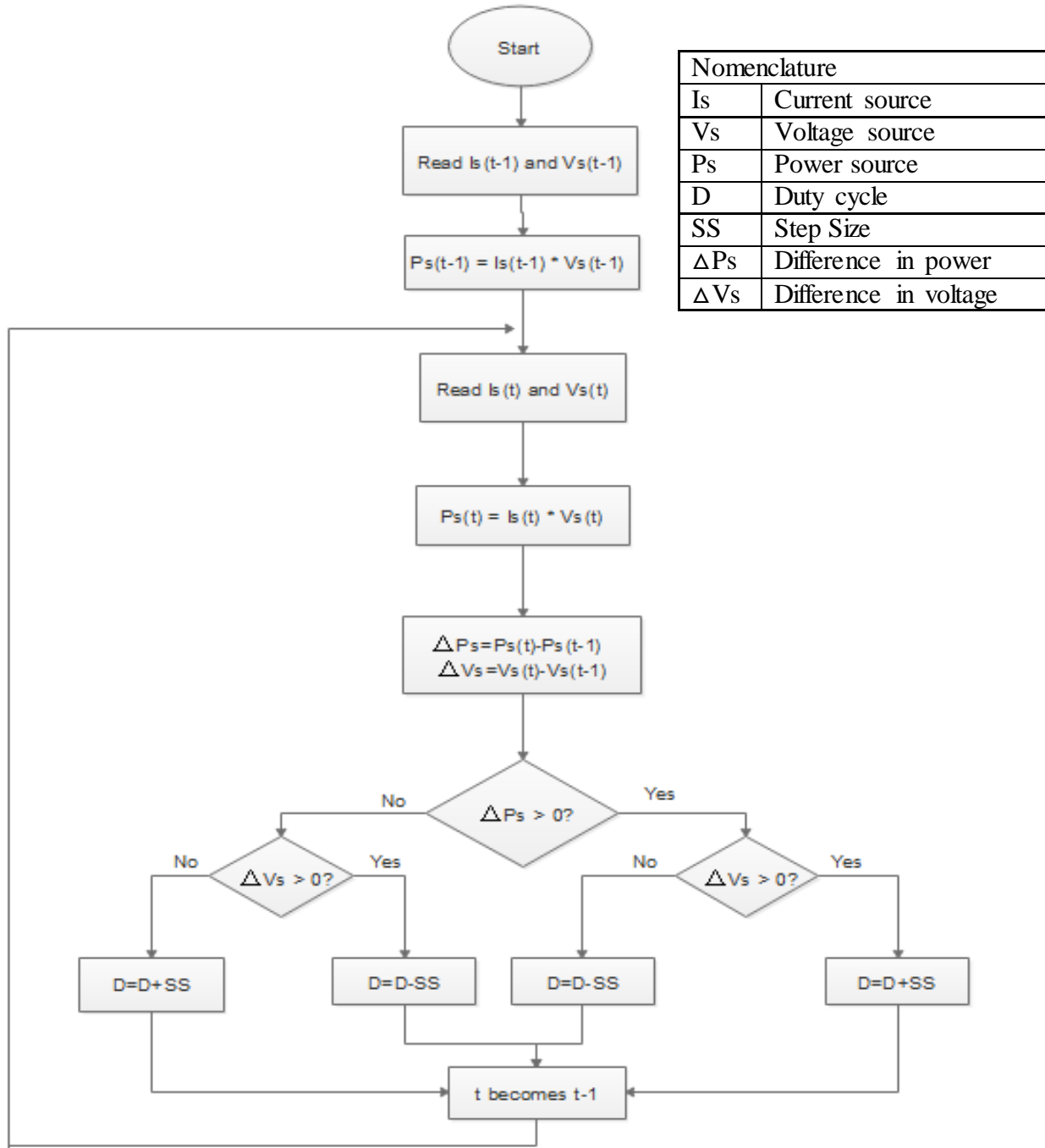


Figure 4.4: Flowchart for Perturb & Observe algorithm modified from (Theoretical and Practical Study of a Photovoltaic MPPT Algorithm Applied to Voltage Battery Regulation, p 85, 2014)

The InC algorithm uses the change of voltage and current instead of the change of power. If the voltage and current do not change, the power does not change because  $P=IxV$ ; which also means if the operating point is in MPP, no change in current and voltage equivalent to no change in duty cycle. InC makes use of the gradient of P-V characteristic curve where if the gradient is zero, means it is at MPP.

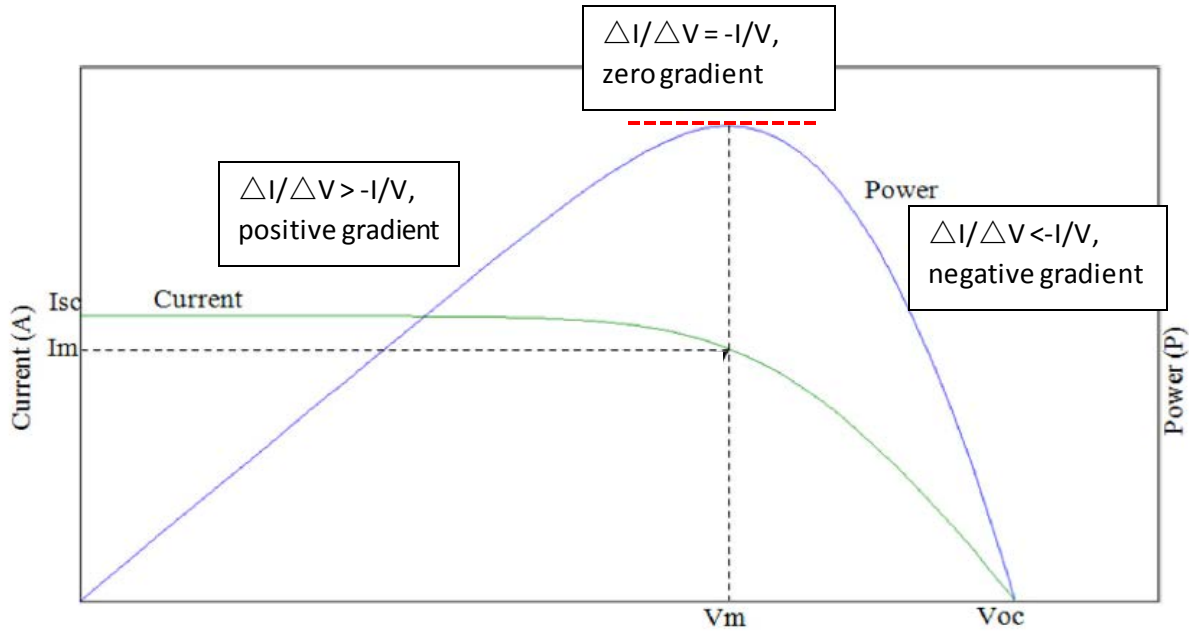


Figure 4.5: The I-V and P-V characteristics curves of a PV module (Solar Panel) modified from Simple and low cost incremental conductance maximum power point tracking using buck-boost converter (2013)

$$\frac{\Delta P}{\Delta V} = \frac{\Delta (I \cdot V)}{\Delta V} = V \frac{\Delta I}{\Delta V} + I \frac{\Delta V}{\Delta V} = V \frac{\Delta V}{\Delta I} + I$$

If  $\Delta P/\Delta V=0$ ; where operating is at MPP, then the equation becomes

$$V \frac{\Delta V}{\Delta I} + I = 0$$

$$\frac{\Delta I}{\Delta V} = -\frac{I}{V}$$

If  $\Delta P/\Delta V > 0$ ; where operating is at the left of MPP, then the equation becomes

$$\frac{\Delta I}{\Delta V} > -\frac{I}{V}$$

If  $\Delta P/\Delta V < 0$ ; where operating is at the right of MPP, then the equation becomes

$$\frac{\Delta I}{\Delta V} < -\frac{I}{V}$$

Using InC, there are 2 ways to determine if the system is working on right operating point in this case, at MPP. One is to use the gradient to determine the current operating point. The other way is to see if there is change of power. The second way is similar to P&O but instead of computing power, the difference between current and voltage is checked. Figure 4.5 shows the flowchart where 2 paths exist to see if the duty cycle needed change. If the operating is at the right of MPP, the duty cycle needs to increase to get nearer to the MPP and vice versa.

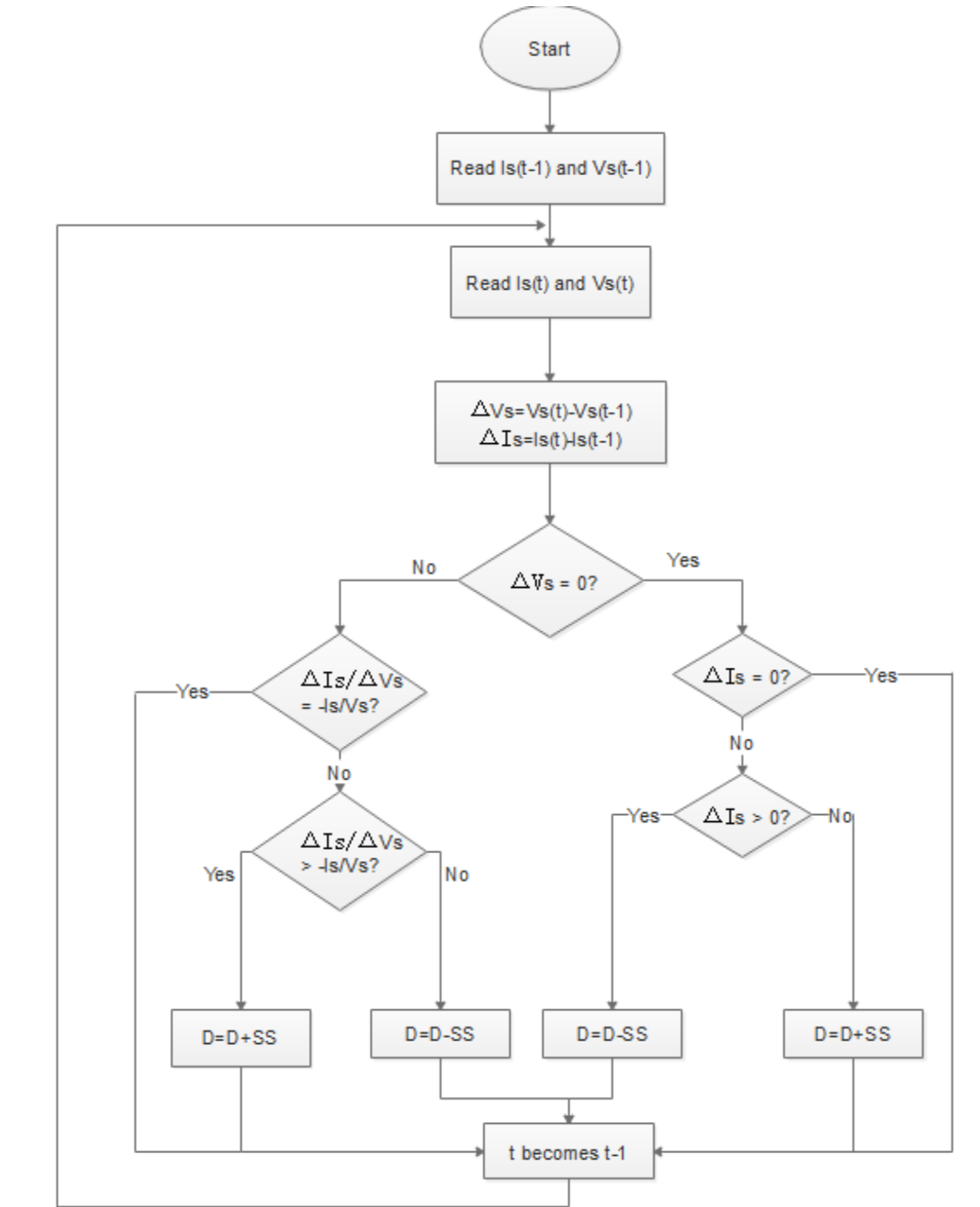


Figure 4.6: Flowchart of Incremental Conductance algorithm modified from (Simple and low cost incremental conductance maximum power point tracking using buck-boost converter, 2013)

There are numerous advantages that InC has compared to P&O. First of all, InC knows if the MPP is reached by checking if  $\Delta P/\Delta V=0$  whereas P&O keeps computing the power and comparing to the previous power value. Even if MPP has reached, P&O keeps oscillating to calculate the power repeatedly. Besides, P&O will keep using power in the microcontroller as the computation is kept running. For InC, computation needs to be done only if there is a change in MPP.

The MPP is yielded when the input and output impedance of the circuit is matched. This can be done by switching the on and off of the MOSFETS at a high frequency. This creates an illusion of a varying impedance. The duty cycle limits the amount of current able to enter the output and this is where the MPPT algorithms comes into play.



## CHAPTER 5: IMPLEMENTATION, TESTING AND ANALYSIS

### 5.0 VERIFICATION PLAN

*Table 5.1: Verification Plan for the system*

<b>TEST TYPE</b>	<b>INPUT</b>	<b>EXPECTED OBSERVATION</b>
<b>ADC – VOLTAGE DIVIDER</b>	Use power supply to pass in 12 V to the voltage divider.	Should observe 2 V at ADC voltage.
<b>CURRENT MEASUREMENT</b>	Use power supply to pass in 0-5 A to the current sensor.	Should observe the corresponding current value after calculation.
<b>PWM FREQUENCY AND DUTY CYCLE</b>	Flash the program into the microcontroller.	Should observe 150Khz and 42% duty cycle using oscilloscope.
<b>BUCK CONVERTER</b>	Install PV module to the buck converter and log the input and output of the buck converter.	Should observe the reduced voltage and increased current as compared to the input.
<b>MPPT ALGORITHMS</b>	Place the algorithm and flash into microcontroller.	Observe the increase or decrease of duty cycle and eventually see the MPP where the LCD backlight turns red at a steady sunlight.
<b>BATTERY CHARGING</b>	Set up the whole circuit to charge the battery.	Able to observe the increase of state of charge in the LCD while powering the microcontroller.

## 5.1 TESTING



Figure 5.2: The oscilloscope showing two pulse wave as verification

A digital oscilloscope is used to verify the duty cycle, frequency and wave form of the gate driver. When the PWM input from the Arduino is supplied, the gate driver outputs 2 pulse wave, one is the inverse of another to be connected to the low side and high side of the MOSFETS. This is to ensure that both MOSFETs does not turn on at the same time or it will result in a short circuit. Since the oscilloscope cannot measure voltage of higher than 5V, digital multimeter is used to measure the average voltage and derive the peak voltage of the pulse wave. For example, if the reading reads 6V in the multimeter from a wave of 50% duty cycle, the peak of the voltage will more or less be 12V.

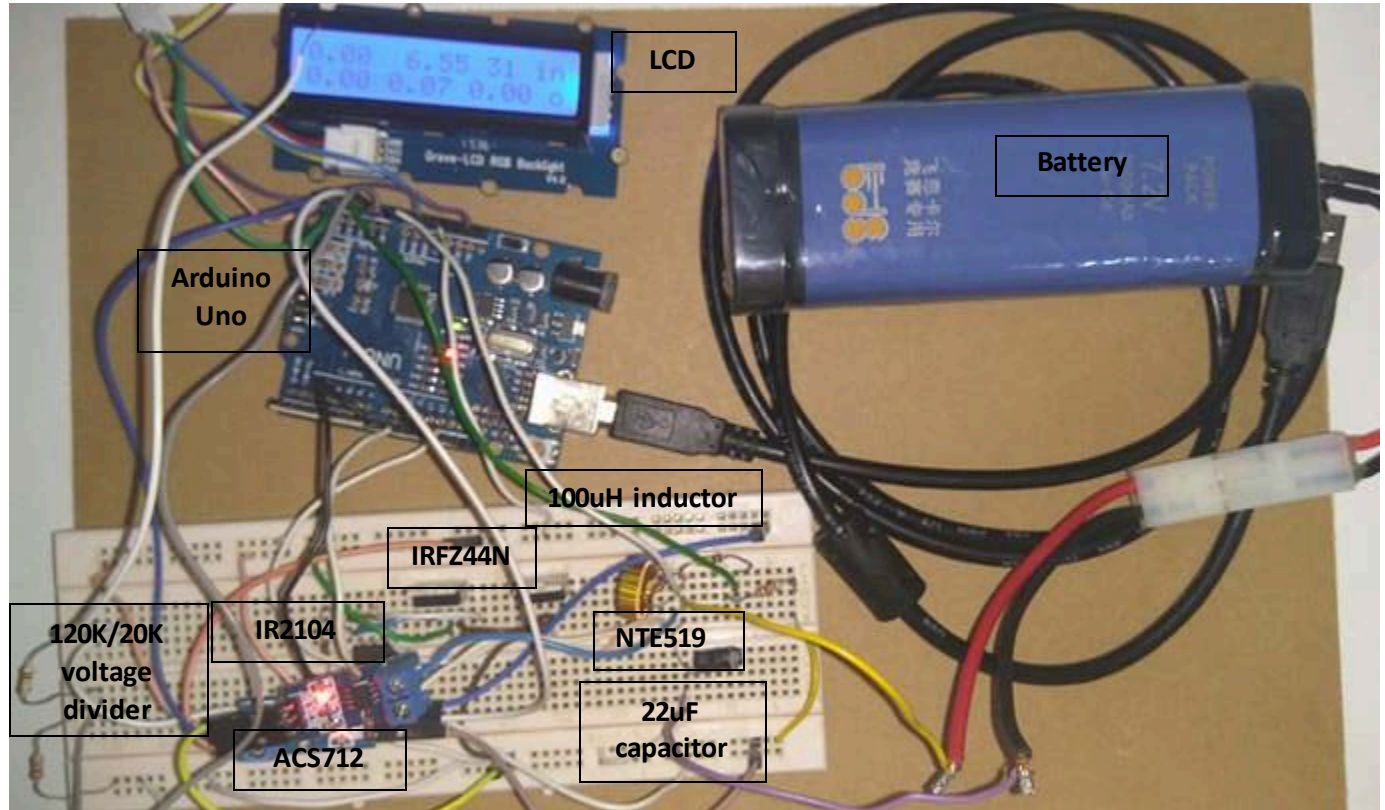


*Figure 5.3: The physical diagram of the system with the battery connected*

The circuit above shows the synchronous buck converter with voltage dividers for voltage measurements and 2 current sensors for input and output current measurements. The microcontroller is powered by the 7.2V NiCd battery. The solar panel is not connected in this picture and therefore showing 0V and 0A on the input side on the LCD.

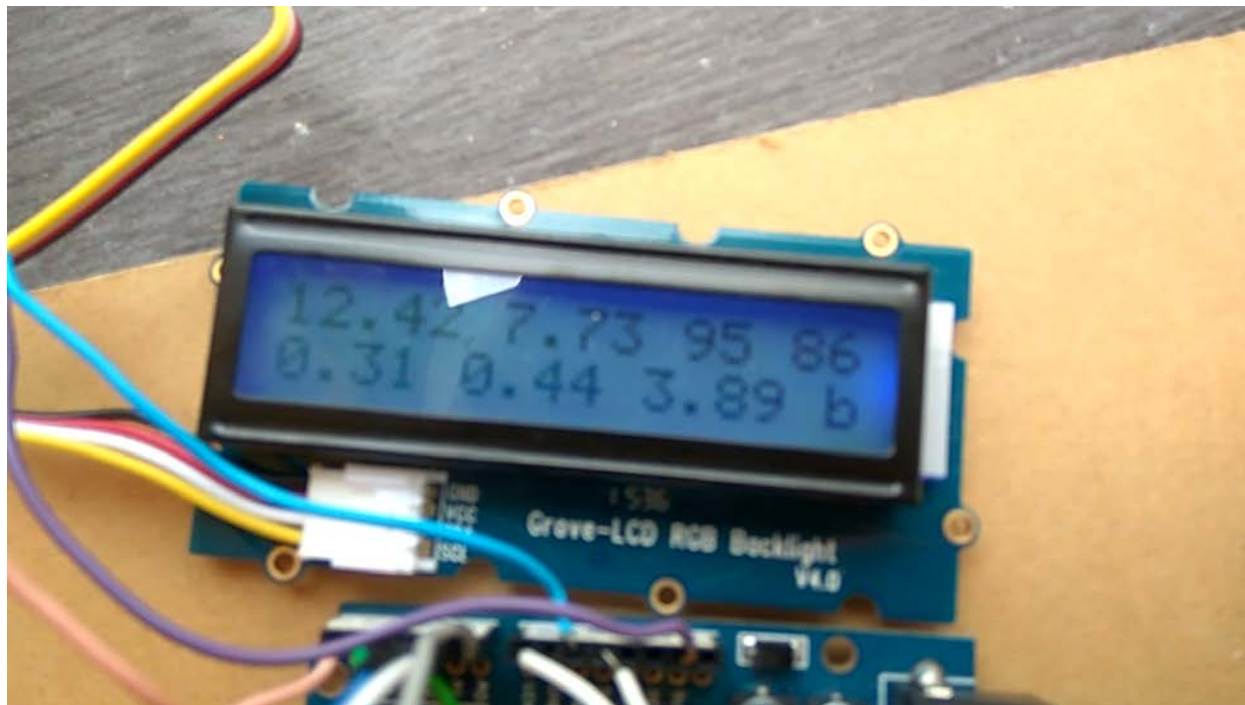


*Figure 5.4: The LCD screen when the system is running*

The LCD display shows the charger working on bulk state (running MPPT algorithm) using a 15W solar panel with the efficiency of 86%. The top left shows the solar voltage and below it shows the solar current. The top middle value is the battery voltage and below it is the current supplied to the battery. The right of the battery voltage is the state of charge of the battery showing 95%. Below it is the current power of the solar panel. This shows the stepped down voltage promised an increased current. This shows that the buck converter is working correctly.

The LCD would also change its backlight color based on the operation state to make the state of the charger more visible. This color is also to verify the correctness of MPPT algorithm since the space in the LCD is limited. The LCD shows the increase or decrease of duty cycle towards MPP and eventually reached the MPP; turning the backlight red. However, due to the changing irradiance of solar panel, the MPP keeps changing and the Power-Voltage characteristic curve is hard to plot.

## 5.2 PRACTICAL VS THEORETICAL EFFICIENCY COMPARISON OF BUCK CONVERTER

$V_{in}=12V$      $V_{out}=5V$     Duty cycle=41.6%    Load=30 ohm

Table 5.5: The efficiency of buck converter under different components and frequency

Calculated switching frequency	Calculated inductor value	Calculated capacitance value	Efficiency in simulation	Efficiency in practical
222 606 Hz →222 222	22 uH	3.93 uF →4.7uF	59.2%	49.5%
103 262 Hz →103 448	47 uH	8.47 uF →10 uF	68%	61.24%
48 533 Hz →48 483	100 uH	18 uF →22 uF	74.8%	70%
485 333 Hz →489 756	10 uH	1.8 uF →2.2 uF	22.7%	18.2%
→150 000 Hz	33 uH	5.83 uF →6.8 uF	64.8%	57%

### EFFICIENCY COMPARISON WITH VARYING SWITCHING FREQUENCY

Table 5.6: Comparison of efficiency on varied frequency in terms of 100 uH inductor value

Switching Frequency	Inductor value	Capacitor value	Efficiency Practical   Simulation
24 266 Hz (-50%) →24 390 Hz-41	100 uH	18 uF -> 22	50-80%   76%
48 533 Hz →47 619 Hz-21	100 uH	18 uF -> 22	40-77%   53%
72 800 Hz (+50%) →71 429 Hz-14	100 uH	18 uF -> 22	40-74%   48%

Table 5.7: Comparison of efficiency on varied frequency in terms of 10 uH inductor value

Switching Frequency	Inductor value	Capacitor value	Efficiency Practical Simulation
242 666 Hz (-50%) →250 000 Hz-4	10 uH	1.8 uF 2.2	19%   36%
485 333 Hz →500 000 Hz-2	10 uH	1.8 2.2 uF	12%   21%
728 000 Hz (+50%) →1 000 000 Hz -1	10 uH	1.8 uF 2.2	Mostly<9 or invalid  12%

*Table 5.8: The state of the charger corresponding to the backlight color of the LCD*

<b>State</b>	<b>Backlight color</b>
OFF	WHITE
ON	GREEN
BULK	BLUE
BULK (REACHED MPP)	RED
FLOAT	GREEN

### 5.3 QUANTIFYING POWER AND EFFICIENCY

#### 5.3.1 POWER CONSUMPTION OF MICROCONTROLLER

As measured by the digital multimeter, the microcontroller consumes the maximum of 0.74W and the minimum of 0.222W. The LCD is actually for debugging and demo purposes. The charger does not need the LCD in the real application.

*Table 5.9: The power consumption of the microcontroller in different conditions*

LCD		Voltage/V	Current/mA	Power/W
CHARACTER	BACKLIGHT			
ON / ON		7.4	100	0.74
ON / OFF		7.4	80	0.592
OFF / OFF		7.4	70	0.518
OFF / OFF (SLEEP)		7.4	30	0.222

#### 5.3.2 REQUIREMENTS FOR MPPT

In order to activate the MPPT algorithm, the solar panel must have minimum power supply of 2W. This is to make sure enough voltage and current are passed in before the manipulation of duty cycle. Any input power between 1W and 2W will result in ON state, where all the available power will be passed to the battery. If the power is below 1W, the charger will be in off state, where no power will be passed to the battery.

#### 5.3.3 EFFICIENCY WITH MPPT

Using the MPPT algorithm Incremental conductance, the efficiency is averagely 70-85% when the battery is still charging at the state of charge of 50-80%. When the charging is almost full, the efficiency increases to high 90s. The efficiency fluctuates around 10% when measuring because of the inaccuracy measurement of the current. As the current measurement has the resolution of 0.026A/step, each step makes huge difference in the power in over power out multiplied by 100.



### 5.3.4 EFFICIENCY WITHOUT MPPT ALGORITHM

The average efficiency is around 37% for partial shading condition. As for fully exposed condition, the charging is extremely slow at the state of charge of below 61% with the charging current of below 0.01A because of the lacked algorithm to track MPP. However, after 61%, the efficiency rises to the 70s and quickly completes the charging. This is because of the absence of MPPT algorithm and the formula used to calculate the duty cycle.

$$PWM = \frac{bat\_volts \times 10}{sol\_volts} + 5$$

This formula is used to approximate the duty cycle of the pulse wave based on the input voltage; *sol\_volts* and output voltage; *bat\_volts*. This formula is used instead of a fixed duty cycle to increase the efficiency and also to compare the differences between a MPPT algorithm and a non-MPPT algorithm.

## 5.4 POWER COMPARISON BETWEEN P&O, InC AND No\_MPPT

### TEST CASES FOR P&O, InC AND No\_MPPT

Table 5.10: The three test cases that have been made against these 3 charging methods.

	Time	Condition	Light intensity/ Lux
<b>Case 1</b>	12pm	Fully exposed	117000
		Partial shading	117000 (covered $\frac{1}{4}$ )
<b>Case 2</b>	10am	Fully exposed	66000
<b>Case 3</b>	5pm	Fully exposed	55000

This is to show the different effects of different algorithm under different sunlight conditions. Each reading is taken with the interval of 500 ms and the solar panel is not moved until all 3 methods of charging are tested. 30 readings are taken for each test and each method.

#### TEST CASE 1: Partial shading results

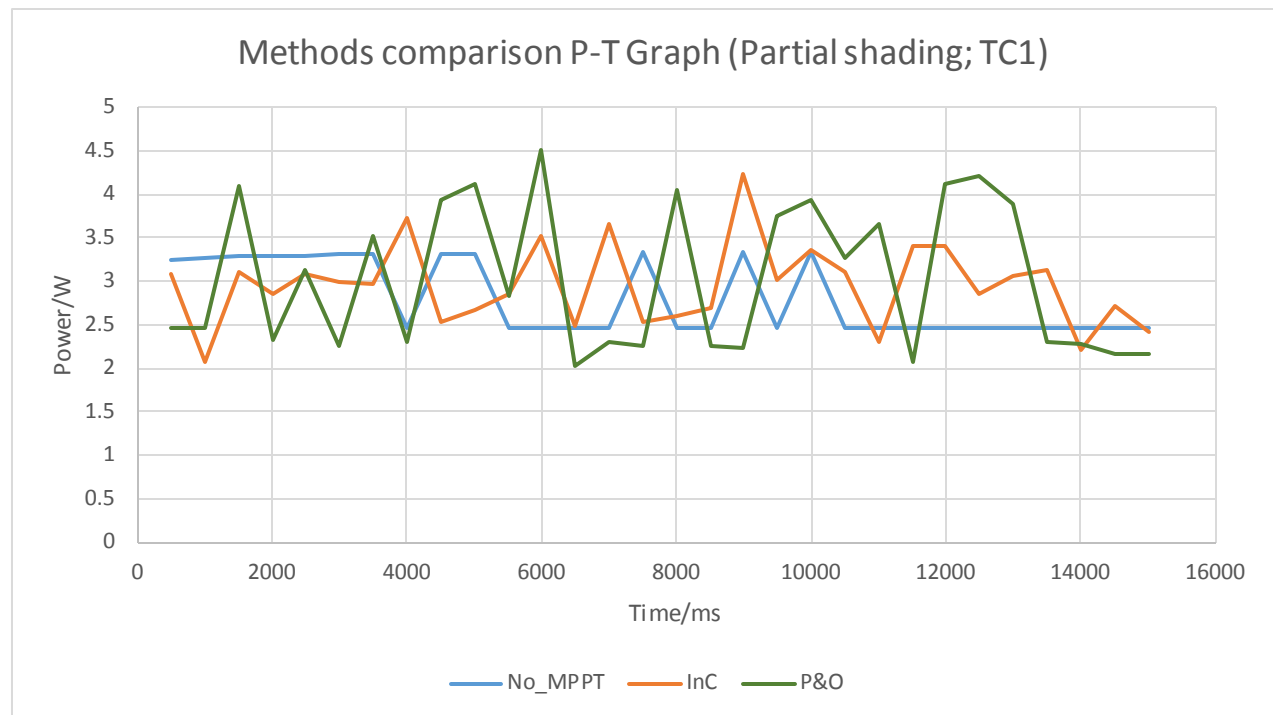
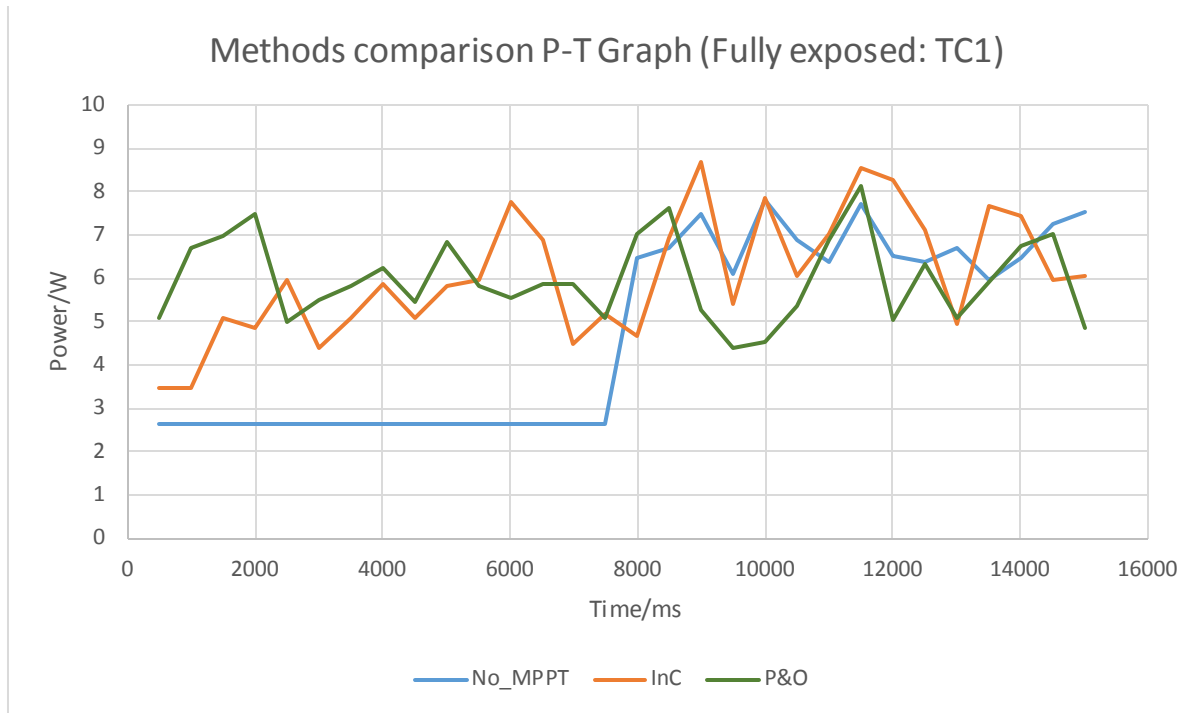


Figure 5.11: The P-T graph of 3 methods under partial shading condition for test case 1

**TEST CASE 1: Fully exposed results**



*Figure 5.12: The P-T graph of 3 methods under fully exposed condition for test case 1*

**TEST CASE 2: Fully exposed results**

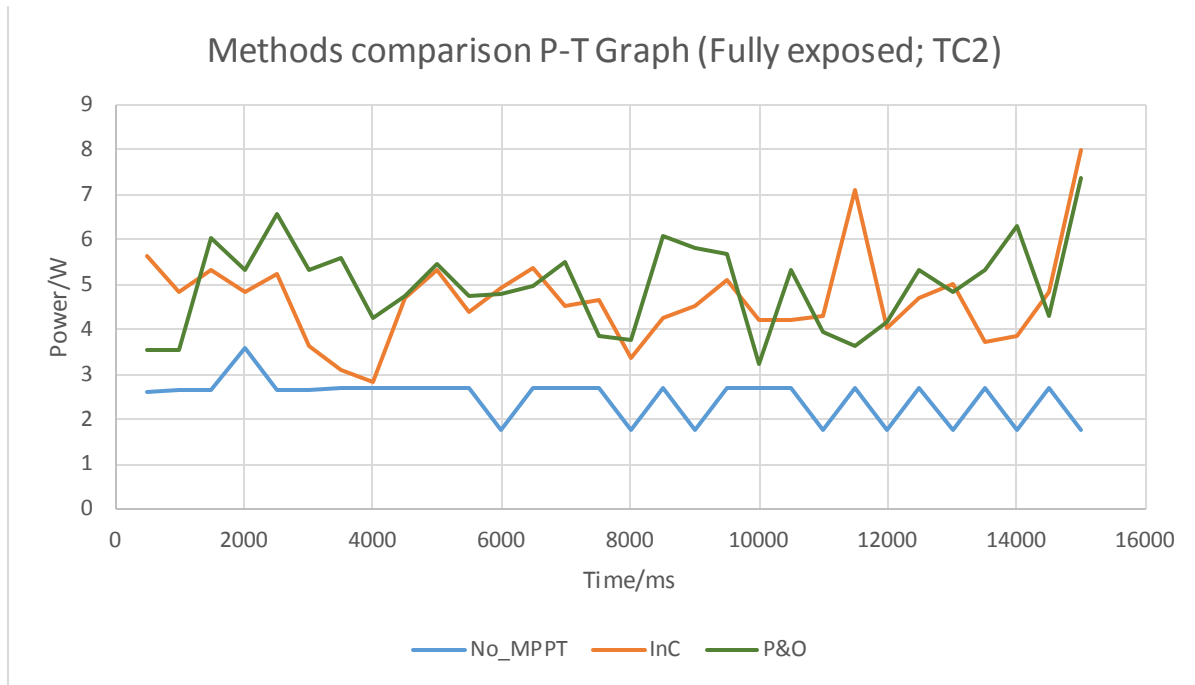


Figure 5.13: The P-T graph of 3 methods under fully exposed condition for test case 2

**TEST CASE 3: Fully exposed results**

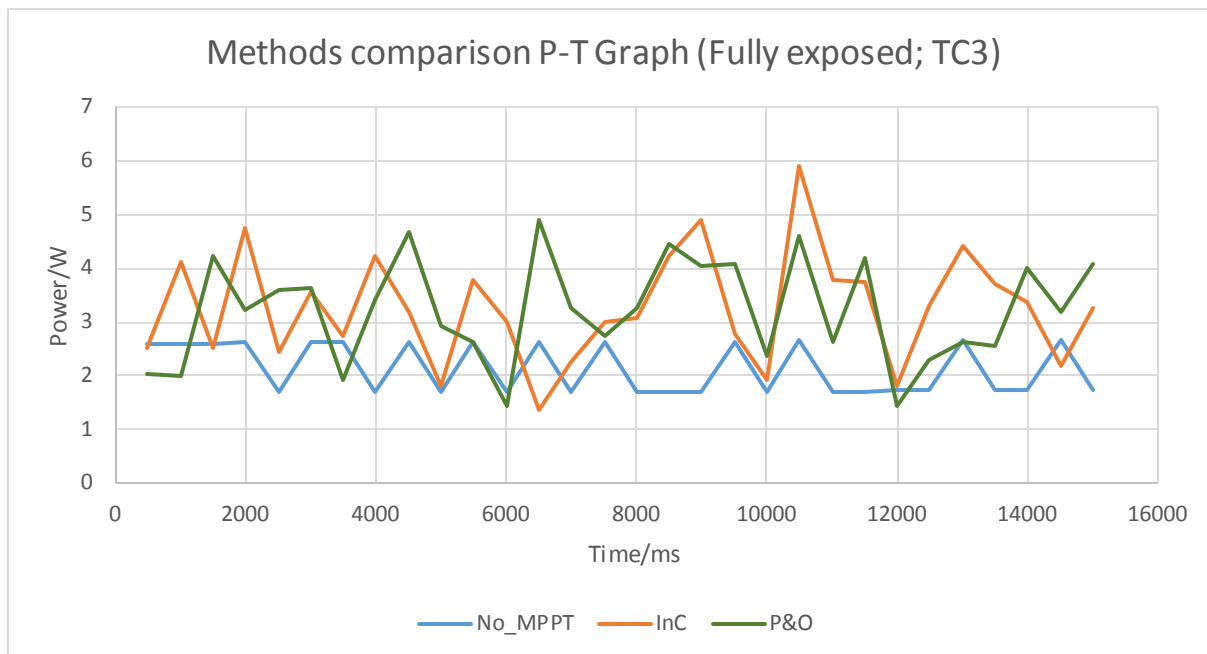


Figure 5.14: The P-T graph of 3 methods under fully exposed condition for test case 3

### 5.5 ANALYSIS OF MPPT ALGORITHMS AND WITHOUT MPPT ALGORITHM

Since there are fluctuations in the solar power, the average output power of the solar panel and energy will be used to see which algorithm works better.

*Table 5.15: The detailed comparison of the three methods of charging tested for test case 1*

<b>TEST CASE 1</b>	<b>InC</b>	<b>P&amp;O</b>	<b>No MPPT algorithm</b>
<b>Average Power (Partial shading) / W</b>	<b>2.95</b>	<b>3.01</b>	<b>2.80</b>
<b>Average Power (Fully exposed) / W</b>	<b>6.06</b>	<b>5.98</b>	<b>4.72</b>
<b>Energy (Partial shading) /J</b>	<b>5.90</b>	<b>6.02</b>	<b>5.60</b>
<b>Energy (Fully exposed) /J</b>	<b>12.12</b>	<b>11.96</b>	<b>9.44</b>
<b>Maximum power point (Partial shading) / W</b>	<b>4.02</b>	<b>4.50</b>	<b>3.72</b>
<b>Maximum power point (Fully exposed) / W</b>	<b>8.69</b>	<b>8.12</b>	<b>7.79</b>
<b>Number of oscillations</b>	<b>Less</b>	<b>More</b>	<b>Least</b>

Under hot sun and fully exposed condition, InC seems to outperform P&O by a little. InC also seem to be able to yield a higher MPP. Both algorithm shows an increase of power of 25-28%. This is shows that the MPPT algorithms implemented really helps in creating a more efficient charger. In partial shading condition, P&O seem to be slightly better than InC. This shows that P&O is a better algorithm to be used if the solar panel will always be blocked by shadows or shade. As for the oscillations or fluctuations, the lesser the better. The method without MPPT algorithm will the most stable as the duty cycle doesn't change every time. This follows by InC which has lesser oscillations because of the calculation to find the MPP. This algorithm can track the real MPP and if it does, the duty cycle will stop and hence no oscillation. However, due to changing irradiance of the solar panel, there will still be fluctuation. The most oscillation will be P&O because of the algorithm's inability to find the exact MPP. This results in always changing duty cycle even though MPP has already achieved.

*Table 5.16: The detailed comparison of the three methods of charging tested for test case 2*

<b>TEST CASE 2</b>	<b>InC</b>	<b>P&amp;O</b>	<b>No MPPT algorithm</b>
<b>Average Power (Fully exposed) / W</b>	<b>4.68</b>	<b>4.97</b>	<b>2.47</b>
<b>Energy (Fully exposed) /J</b>	<b>9.36</b>	<b>9.94</b>	<b>4.94</b>
<b>Maximum power point (Fully exposed) / W</b>	<b>8.00</b>	<b>7.38</b>	<b>3.60</b>
<b>Number of oscillations</b>	<b>Moderate</b>	<b>Moderate</b>	<b>Least</b>

As for test case 2, P&O seems to be a little better under lower sunlight condition than InC. This may be because of the ability of P&O that can track MPP faster than InC. If the MPP is tracked faster, the overall power output may be higher even if there are more oscillations on the output. But for this case, the oscillation for both P&O and InC seems to be more or less the same. This leads to better power output for P&O. Even so, InC is still able to yield a higher MPP. As for without MPPT algorithm, it has the most stable power output but because of the inability to track MPP, its average power output is the lowest compared to the other two at 2.47W.

*Table 5.17: The detailed comparison of the three methods of charging tested for test case 3*

<b>TEST CASE 3</b>	<b>InC</b>	<b>P&amp;O</b>	<b>No MPPT algorithm</b>
<b>Average Power (Fully exposed) / W</b>	<b>3.26</b>	<b>3.21</b>	<b>2.14</b>
<b>Energy (Fully exposed) /J</b>	<b>6.52</b>	<b>6.42</b>	<b>4.28</b>
<b>Maximum power point (Fully exposed) / W</b>	<b>5.90</b>	<b>4.80</b>	<b>1.72</b>
<b>Number of oscillations</b>	<b>Moderate</b>	<b>Moderate</b>	<b>Least</b>

In this comparison, InC seems to be a little better than P&O in MPP and average power. Test case 3 has the lowest light intensity comparing to the other two cases, this shows that InC works better in lower light conditions. The oscillations for P&O and InC are around the same and no MPPT algorithm has the least number of oscillations.

## **SUMMARY OF ANALYSIS**

As a summary, InC always yields a higher MPP but InC and P&O might outperform one another in different cases. InC works better in very bright and very shady weather according to the data obtained. P&O is better in moderate not too bright and not too shady sunlight conditions. P&O always have more or equal oscillations comparing to InC. The efficiency comparison of these 2 algorithms is unable to compute as the efficiency value fluctuates a lot. However, the fluctuation of both the algorithms are almost the same. The efficiencies are fluctuation above 70% most of the time. Therefore, the average power is used instead, to see how good those algorithm perform. The no MPPT algorithm proves to be the worst among all 3 because of its inability to track MPP.

### Factors that Results to Inaccuracy of Data

Three methods of charging are tested one after another. The data might not be exactly the same as tested as before because the sunlight and clouds will not be exactly the same. Due to the changing irradiance of sunlight, the solar power fluctuates a lot as the duty cycle changes. This happens more using P&O as the algorithm because it cannot track the true MPP. Hence, even if it found the MPP, there will still be oscillations around the MPP. The InC has the capability of finding the true MPP using the gradient formula of the P-V graph of the solar panel which results in a lesser oscillation.

## 5.6 ISSUES AND CHALLENGES

Since the microcontroller is powered by the battery that the buck converter charges, the microcontroller needs to be able to provide PWM for the buck converter to work. If the microcontroller does not have power, there would be no PWM and no switching frequency. No switching means the gate of MOSFET will not turn on. Then, the buck converter will not be able to work at all because current cannot flow to inductor and then capacitor. Therefore, the battery must always contain sufficient power to support the operation of this system.

Another problem is that the buck converter needs to be able to charge the battery faster than the battery gets discharge by the microcontroller. If not, the system will stop working after sometime because there is no more charges left on the battery. In order to avoid this problem, the buck converter must be as efficient as possible and the microcontroller must use as little power as possible.

The use of MSP432 has been change to Arduino Uno due to some pin voltage tolerance problem. Many pins of the MSP432 have been damaged because of a faulty gate driver that outputs 5V in an input pin. Based on the datasheet of MSP432, the GPIO pins can only accept a maximum of 4.4V where 5V that comes from the SD' pin is somehow leaked to the input pin IN and damaged the microcontroller. Due to limited budget and time, I found that this microcontroller is not really suitable for this project unless this project is a group project and people with more knowledge of power electronics are involved.

One powerbank is completed damaged when the supply current is around 1.5A where its rated current is 1A. This may be because the powerbank does not have overcurrent protection circuit. The battery and solar panel must be selected very carefully because any mismatch will result in either parts burned or damaged.



## 5.7 SOLUTION TO PROBLEM

The battery must have a little charge to power up the microcontroller before starting the system. This is to supply power to the microcontroller and the microcontroller will supply pulse wave to the gate driver. Besides, the LCD backlight can be disabled or the LCD can be removed to further reduce the power consumption of the microcontroller. The LCD is only there for verification purpose.

In order to sustain the power supply to the microcontroller and battery, a larger PV module with higher power can be used. However, the microcontroller must be capable of sensing a larger range of voltage and current from the PV module.

A Ni-Cd battery is used to replace the powerbank as batteries like these are more forgiving on the voltage and current supplied. They do not explode like lithium ion batteries that are used in powerbanks.

## 5.8 LIMITATIONS

Since the Arduino uno is more of a general purpose microcontroller, the peripherals and resolution of the ADC is limited. This results in less accurate measurements that influences the efficiency and computation power.

This system is un-tolerable to heat. During the charging, it is best for the system to stay indoors. Heat may reduce the overall efficiency of the buck converter. Other problem like damaged component in a long term run may arise as well with heat.

This system has lacked intelligence to switch off the microcontroller when the charge is completed. This could not be implemented as there is time constraint on this project.

### 5.9 TIMELINE

The buck converter design has taken 1 semester together with various measurements.

#### GANTT CHART FOR FYP 1

FYP 1	WEEK													
	1	2	3	4	5	6	7	8	9	10	11	12	13	14
Configure PWM	█	█												
Configure ADC			█	█										
Set up potentiometer					█									
Set up current sensor						█								
Build buck converter circuit							█	█						
Testing buck converter circuit									█	█				
Combining measurement and buck converter											█			
Verification of the whole system												█	█	
Submission														█

**GANTT CHART FOR FYP 2**

The implementation of MPPT algorithm took 1 semester to complete as the algorithm would need a lot of testing. The whole system is completed.

FYP 2	WEEK													
	1	2	3	4	5	6	7	8	9	10	11	12	13	14
Install PV module	■	■												
Configure MPPT algorithm			■	■										
Verification of MPPT algorithm					■	■	■	■						
Verification of whole system									■	■				
Computing efficiency of system											■	■		
Comparison of 2 algorithms													■	
Submission														■

## CHAPTER 6: CONCLUSION

### 6.1 PROJECT REVIEW

A solar charger with the capability of tracking the MPP have been build. Analysis of different types of circuit, components, hardware and algorithms has been made based on how efficiency is affected. To build this system, it requires knowledge of power electronics, circuit theory, solar panel and lithium ion/nickel cadmium battery characteristics, software knowledge; to program the microcontroller, the understanding of microcontroller on how peripherals and features are used based on the specification of the microcontroller. Last but not least, the skill of troubleshooting is very much needed to identify the root of problem when one is encountered, whether it's a problem with component, concept, microcontroller, software logic or a loose wire connection.

Many problems have been faced and the largest regret is the change of microcontroller (MSP432) to Arduino Uno. After many tests, research and time spent on implementing MSP432 with the system, just to find that the microcontroller is not suitable for the system due to the microcontroller's tolerance to damage, complexity in programming and also the cost for the microcontroller. It is not impossible for the MSP432 to be implemented with the system, it is just that a team of people with better knowledge in power electronics, has more time and higher budget would be more suitable.

## 6.2 FURTHER IMPROVEMENTS IN FUTURE

Many improvements can still be made to the system. A solar panel with micro-inverter and a lower powered microcontroller can be used together to further improve the charging, efficiency and speed of the system. Micro-inverter solar panels have better efficiency under partial shading condition. This leads to higher power output in or out of shadow on the solar panel. Implementation in PCB (Printed Circuit Board) would be useful as it eliminates the poor conduction of electricity in wires.

One of the biggest problem in this project is that the absence of many protection which can lead to damaged components. Protection can be of short circuit, high current, reverse electricity protection, low voltage disconnect, etc. Therefore, the charger in the future can be made to protect itself.

Instead of using only sleep, the microcontroller can be completely turned off. This feature have been tried to be implemented but the circuit constructed seems to have problem. The 5V from the digital pin cannot seem to turn on the logic level MOSFET unless an external 5V is used.

Lastly, this system can be modified to support larger solar panel with higher power and a battery with larger capacity, capable in powering multiple loads. The load can be of any device with an external voltage regulator built in on the system that can be controlled by the user to charge any device.

### **6.3 FINAL REMARK**

The reliance of non-renewable energy in the world today needs to be changed. Sooner or later, these sources would be depleted. This project can be further improve by adding more renewable energy source to increase the input power and speed up the charging of battery. Other DC-DC converter can be used to step up or step down the voltage when needed. The buck-boost converter can be used but the circuit and the microcontroller programming would be more complex. This project is the first step in creating a self-sustainable system and also to charge a battery which can be used to power any device with a voltage regulator; especially IoT device.

## REFERENCES

- Enerdata. (2014). 'Total energy consumption' [online]. Available from <https://yearbook.enerdata.net/#energy-consumption-data.html> (Accessed 1 April 2016)
- BU-409: *Charging Lithium-ion* (2016) [online]. Available from [http://batteryuniversity.com/learn/article/charging\\_lithium\\_ion\\_batteries](http://batteryuniversity.com/learn/article/charging_lithium_ion_batteries) (Accessed 1 April 2016)
- Tey,KS et. al (2013). 'Simple and low cost incremental conductance maximum power point tracking using buck-boost converter', AIP Publishing [online], pp.2,5, 7 March. Available from <http://repository.um.edu.my/30658/1/Simple%20and%20low%20cost%20incremental%20conductance%20maximum.pdf>(Accessed 1 April 2016)
- Source Resistance: *The Efficiency Killer in DC-DC Converter Circuits* (2004) [online], p 1. Available from <https://www.maximintegrated.com/en/app-notes/index.mvp/id/3166>(Accessed 28 March 2016)
- Keeping,S (2014). 'The SEPIC Option for Battery-Power Management' [online]. Available from <http://www.digikey.com/en/articles/techzone/2014/aug/the-sepic-option-for-battery-power-management>(Accessed 27 March 2016)
- Switched Mode Power Supplies* [online], pp. 4,7,10. Available from <http://www.learnabout-electronics.org/PSU/psu30.php>(Accessed 27 March 2016)
- Sher.HA et. al (2015). 'A New Sensorless Hybrid MPPT Algorithm Based On Fractional Short-Circuit Current Measurement and P&O MPPT', IEEE Transactions on Sustainable Energy, Vol. 6, No. 4, October, pp.1426-1428.
- Amara.S et. al (2014). 'Theoretical and Practical Study of a Photovoltaic MPPT Algorithm Applied to Voltage Battery Regulation', International Journal of Renewable Energy Research, Vol. 4, No.1, 2014, pp. 84-89.

Ashraf.A et. al (2013). 'A Fast PV Power Tracking Control Algorithm With Reduced Power Mode', IEEE Transactions on Energy Conversion, Vol. 28, No. 3, September 2013, pp. 565-574.

Cooper.C (2013). 'Fundamentals of Buck Converter Efficiency' [online]. Available from <http://electronicdesign.com/power/fundamentals-buck-converter-efficiency>(Accessed 28 March 2016)

Nowakowski.R et. al (2006). 'Choosing the optimum switching frequency of your DC/DC converter'[online]. Available from [http://www.eetimes.com/document.asp?doc\\_id=1272335](http://www.eetimes.com/document.asp?doc_id=1272335)(Accessed 28 March 2016)

Mankar.PU, Moharil.RM (2014). 'Comparative Analysis Of The Perturb-and-Observe and Perturb-And-Observe and Incremental' [online], International Journal of Research in Engineering and Applied Sciences, p 60. Available from [www.mgijournal.com/pdf\\_new/Electrical/Prateek%20mankar.pdf](http://www.mgijournal.com/pdf_new/Electrical/Prateek%20mankar.pdf)(Accessed 28 March 2016)

Moubayed.N et. al (2009). 'A comparison of two MPPT techniques for PV system' [online]. WSEAS TRANSACTIONS on ENVIRONMENT and DEVELOPMENT, Issue 12. Vol. 5, December, p 778. Available from <http://www.wseas.us/e-library/transactions/environment/2009/32-603.pdf>(Accessed 27 March 2016).

'LC Selection Guide for the DC-DC Synchronous Buck Converter' [online] (2013). AND9135/D, p 7. Available from [www.onsemi.com/pub/Collateral/AND9135-D.PDF](http://www.onsemi.com/pub/Collateral/AND9135-D.PDF)(Accessed 26 March 2016).

Apps Support (2013). 'Back to Basics: The Importance of Switching Frequency' [online], September 30. Available from <http://powerblog.vicorpower.com/2013/09/back-to-basics-the-importance-of-switching-frequency/>(Accessed 26 March 2016).



## APPENDICES

### APPENDIX A

Datasheet of IR2104

International  
**IR** Rectifier

Data Sheet No. PD60046-S

## IR2104(S) & (PbF)

### HALF-BRIDGE DRIVER

#### Features

- Floating channel designed for bootstrap operation Fully operational to +600V Tolerant to negative transient voltage dV/dt immune
- Gate drive supply range from 10 to 20V
- Undervoltage lockout
- 3.3V, 5V and 15V input logic compatible
- Cross-conduction prevention logic
- Internally set deadtime
- High side output in phase with input
- Shut down input turns off both channels
- Matched propagation delay for both channels
- Also available LEAD-FREE

#### Description

The IR2104(S) are high voltage, high speed power MOSFET and IGBT drivers with dependent high and low side referenced output channels. Proprietary HVIC and latch immune CMOS technologies enable ruggedized monolithic construction. The logic input is compatible with standard CMOS or LSTTL output, down to 3.3V logic. The output drivers feature a high pulse current buffer stage designed for minimum driver cross-conduction. The floating channel can be used to drive an N-channel power MOSFET or IGBT in the high side configuration which operates from 10 to 600 volts.

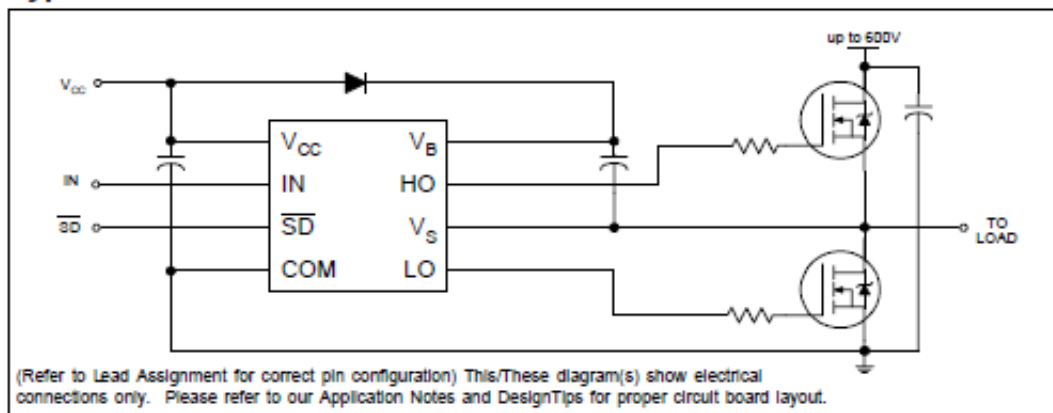
#### Product Summary

$V_{\text{OFFSET}}$	600V max.
$I_{\text{O}+/-}$	130 mA / 270 mA
$V_{\text{OUT}}$	10 - 20V
$t_{\text{on/off}}$ (typ.)	680 & 150 ns
Deadtime (typ.)	520 ns

#### Packages



#### Typical Connection



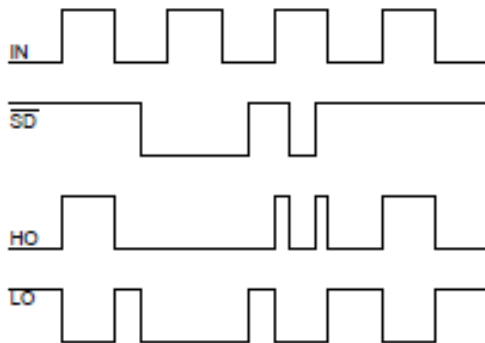


Figure 1. Input/Output Timing Diagram

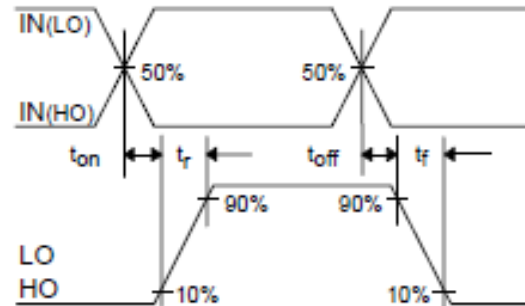


Figure 2. Switching Time Waveform Definitions

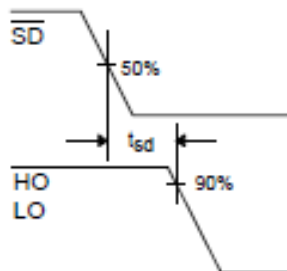


Figure 3. Shutdown Waveform Definitions

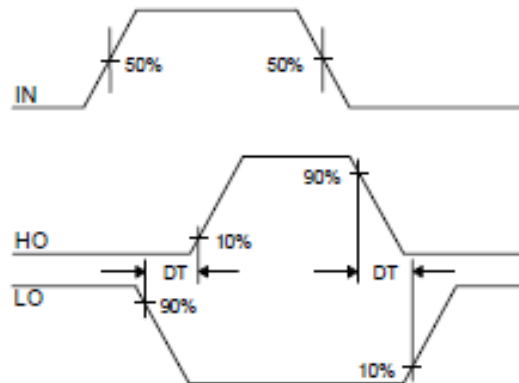


Figure 4. Deadtime Waveform Definitions

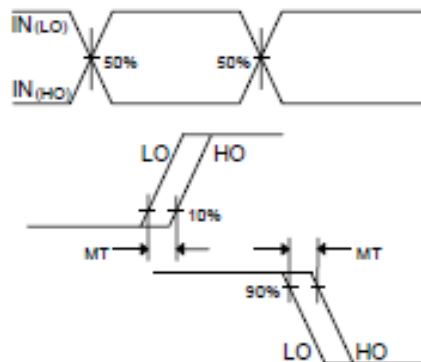


Figure 5. Delay Matching Waveform Definitions

**APPENDIX B**

Datasheet of IRFZ44N

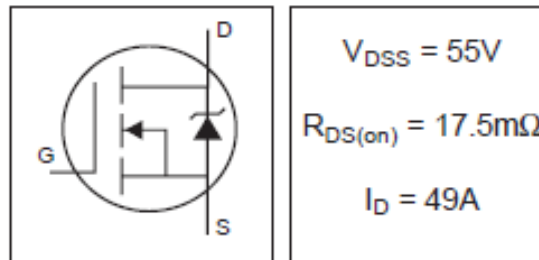


PD - 94053

**IRFZ44N**

HEXFET® Power MOSFET

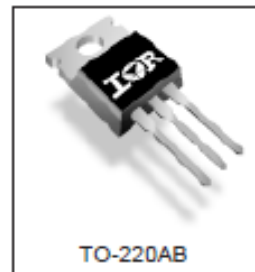
- Advanced Process Technology
- Ultra Low On-Resistance
- Dynamic dv/dt Rating
- 175°C Operating Temperature
- Fast Switching
- Fully Avalanche Rated



**Description**

Advanced HEXFET® Power MOSFETs from International Rectifier utilize advanced processing techniques to achieve extremely low on-resistance per silicon area. This benefit, combined with the fast switching speed and ruggedized device design that HEXFET power MOSFETs are well known for, provides the designer with an extremely efficient and reliable device for use in a wide variety of applications.

The TO-220 package is universally preferred for all commercial-industrial applications at power dissipation levels to approximately 50 watts. The low thermal resistance and low package cost of the TO-220 contribute to its wide acceptance throughout the industry.



**Absolute Maximum Ratings**


	Parameter	Max.	Units
$I_D @ T_C = 25^\circ C$	Continuous Drain Current, $V_{GS} @ 10V$	49	A
$I_D @ T_C = 100^\circ C$	Continuous Drain Current, $V_{GS} @ 10V$	35	
$I_{DM}$	Pulsed Drain Current ①	180	
$P_D @ T_C = 25^\circ C$	Power Dissipation	94	W
	Linear Derating Factor	0.63	W/°C
$V_{GS}$	Gate-to-Source Voltage	$\pm 20$	V
$I_{AR}$	Avalanche Current ①	25	A
$E_{AR}$	Repetitive Avalanche Energy ①	9.4	mJ
dv/dt	Peak Diode Recovery dv/dt ②	5.0	V/ns
$T_J$	Operating Junction and	-55 to +175	°C
$T_{STG}$	Storage Temperature Range		
	Soldering Temperature, for 10 seconds	300 (1.6mm from case )	
	Mounting torque, 6-32 or M3 screw	10 lbf-in (1.1N-m)	

**Thermal Resistance**

	Parameter	Typ.	Max.	Units
$R_{\theta JC}$	Junction-to-Case	—	1.5	°C/W
$R_{\theta CS}$	Case-to-Sink, Flat, Greased Surface	0.50	—	
$R_{\theta JA}$	Junction-to-Ambient	—	62	

## APPENDIX C

### Datasheet of ATmega328



## ATmega48A/PA/88A/PA/168A/PA/328/P

---

### ATMEL 8-BIT MICROCONTROLLER WITH 4/8/16/32KBYTES IN-SYSTEM PROGRAMMABLE FLASH

**DATASHEET**

#### Features

---

- High Performance, Low Power Atmel®AVR® 8-Bit Microcontroller Family
- Advanced RISC Architecture
  - 131 Powerful Instructions – Most Single Clock Cycle Execution
  - 32 x 8 General Purpose Working Registers
  - Fully Static Operation
  - Up to 20 MIPS Throughput at 20MHz
  - On-chip 2-cycle Multiplier
- High Endurance Non-volatile Memory Segments
  - 4/8/16/32KBytes of In-System Self-Programmable Flash program memory
  - 256/512/512/1KBytes EEPROM
  - 512/1K/1K/2KBytes Internal SRAM
  - Write/Erase Cycles: 10,000 Flash/100,000 EEPROM
  - Data retention: 20 years at 85°C/100 years at 25°C<sup>(1)</sup>
  - Optional Boot Code Section with Independent Lock Bits
    - In-System Programming by On-chip Boot Program
    - True Read-While-Write Operation
  - Programming Lock for Software Security
- Atmel® QTouch® library support
  - Capacitive touch buttons, sliders and wheels
  - QTouch and QMatrix® acquisition
  - Up to 64 sense channels
- Peripheral Features
  - Two 8-bit Timer/Counters with Separate Prescaler and Compare Mode
  - One 16-bit Timer/Counter with Separate Prescaler, Compare Mode, and Capture Mode
  - Real Time Counter with Separate Oscillator
  - Six PWM Channels
  - 8-channel 10-bit ADC in TQFP and QFN/MLF package
    - Temperature Measurement
  - 6-channel 10-bit ADC in PDIP Package
    - Temperature Measurement
  - Programmable Serial USART
  - Master/Slave SPI Serial Interface
  - Byte-oriented 2-wire Serial Interface (Philips I<sup>2</sup>C compatible)
  - Programmable Watchdog Timer with Separate On-chip Oscillator
  - On-chip Analog Comparator
  - Interrupt and Wake-up on Pin Change

## 10. Power Management and Sleep Modes

Sleep modes enable the application to shut down unused modules in the MCU, thereby saving power. The AVR provides various sleep modes allowing the user to tailor the power consumption to the application's requirements.

When enabled, the Brown-out Detector (BOD) actively monitors the power supply voltage during the sleep periods. To further save power, it is possible to disable the BOD in some sleep modes. See "BOD Disable(1)" on page 40 for more details.

### 10.1 Sleep Modes

Figure 9-1 on page 27 presents the different clock systems in the ATmega48A/PA/88A/PA/168A/PA/328/P, and their distribution. The figure is helpful in selecting an appropriate sleep mode. Table 10-1 shows the different sleep modes, their wake up sources BOD disable ability.<sup>(1)</sup>

Note: 1. BOD disable is only available for ATmega48PA/88PA/168PA/328P.

Table 10-1. Active Clock Domains and Wake-up Sources in the Different Sleep Modes.

	Active Clock Domains					Oscillators			Wake-up Sources						Software BOD Disable
	clk <sub>CPU</sub>	clk <sub>FLASH</sub>	clk <sub>IO</sub>	clk <sub>ADC</sub>	clk <sub>ASY</sub>	Main Clock Source Enabled	Timer Oscillator Enabled	INT1, INT0 and Pin Change	TW Address Match	Timer2	SPM/EEPROM Ready	ADC	WDT	Other I/O	
Idle			X	X	X	X	X <sup>(2)</sup>	X	X	X	X	X	X	X	
ADC Noise Reduction				X	X	X	X <sup>(2)</sup>	X <sup>(3)</sup>	X	X <sup>(2)</sup>	X	X	X		
Power-down								X <sup>(3)</sup>	X				X		X
Power-save					X		X <sup>(2)</sup>	X <sup>(3)</sup>	X	X			X		X
Standby <sup>(1)</sup>						X		X <sup>(3)</sup>	X				X		X
Extended Standby					X <sup>(2)</sup>	X	X <sup>(2)</sup>	X <sup>(3)</sup>	X	X			X		X

Notes: 1. Only recommended with external crystal or resonator selected as clock source.  
 2. If Timer/Counter2 is running in asynchronous mode.  
 3. For INT1 and INT0, only level interrupt.

To enter any of the six sleep modes, the SE bit in SMCR must be written to logic one and a SLEEP instruction must be executed. The SM2, SM1, and SM0 bits in the SMCR Register select which sleep mode (Idle, ADC Noise Reduction, Power-down, Power-save, Standby, or Extended Standby) will be activated by the SLEEP instruction. See Table 10-2 on page 44 for a summary.

If an enabled interrupt occurs while the MCU is in a sleep mode, the MCU wakes up. The MCU is then halted for four cycles in addition to the start-up time, executes the interrupt routine, and resumes execution from the instruction following SLEEP. The contents of the Register File and SRAM are unaltered when the device wakes up from sleep. If a reset occurs during sleep mode, the MCU wakes up and executes from the Reset Vector.

## 16. 16-bit Timer/Counter1 with PWM

### 16.1 Features

- True 16-bit Design (i.e., Allows 16-bit PWM)
- Two independent Output Compare Units
- Double Buffered Output Compare Registers
- One Input Capture Unit
- Input Capture Noise Canceler
- Clear Timer on Compare Match (Auto Reload)
- Glitch-free, Phase Correct Pulse Width Modulator (PWM)
- Variable PWM Period
- Frequency Generator
- External Event Counter
- Four independent interrupt Sources (TOV1, OCF1A, OCF1B, and ICF1)

### 16.2 Overview

The 16-bit Timer/Counter unit allows accurate program execution timing (event management), wave generation, and signal timing measurement.

Most register and bit references in this section are written in general form. A lower case "n" replaces the Timer/Counter number, and a lower case "x" replaces the Output Compare unit channel. However, when using the register or bit defines in a program, the precise form must be used, i.e., TCNT1 for accessing Timer/Counter1 counter value and so on.

A simplified block diagram of the 16-bit Timer/Counter is shown in [Figure 16-1](#). For the actual placement of I/O pins, refer to "[Pinout ATmega48A/PA/88A/PA/168A/PA/328/P](#)" on [page 3](#). CPU accessible I/O Registers, including I/O bits and I/O pins, are shown in bold. The device-specific I/O Register and bit locations are listed in the "[Register Description](#)" on [page 131](#).

The PRTIM1 bit in "[PRR – Power Reduction Register](#)" on [page 45](#) must be written to zero to enable Timer/Counter1 module.

## 24. Analog-to-Digital Converter

### 24.1 Features

- 10-bit Resolution
- 0.5 LSB Integral Non-linearity
- $\pm 2$  LSB Absolute Accuracy
- 13 - 260 $\mu$ s Conversion Time
- Up to 76.9kSPS (Up to 15kSPS at Maximum Resolution)
- 6 Multiplexed Single Ended Input Channels
- 2 Additional Multiplexed Single Ended Input Channels (TQFP and QFN/MLF Package only)
- Temperature Sensor Input Channel
- Optional Left Adjustment for ADC Result Readout
- 0 -  $V_{CC}$  ADC Input Voltage Range
- Selectable 1.1V ADC Reference Voltage
- Free Running or Single Conversion Mode
- Interrupt on ADC Conversion Complete
- Sleep Mode Noise Canceler

### 24.2 Overview

The ATmega48A/PA/88A/PA/168A/PA/328/P features a 10-bit successive approximation ADC. The ADC is connected to an 8-channel Analog Multiplexer which allows eight single-ended voltage inputs constructed from the pins of Port A. The single-ended voltage inputs refer to 0V (GND).

The ADC contains a Sample and Hold circuit which ensures that the input voltage to the ADC is held at a constant level during conversion. A block diagram of the ADC is shown in [Figure 24-1 on page 238](#).

The ADC has a separate analog supply voltage pin,  $AV_{CC}$ .  $AV_{CC}$  must not differ more than  $\pm 0.3V$  from  $V_{CC}$ . See the paragraph "[ADC Noise Canceler](#)" on page 243 on how to connect this pin.

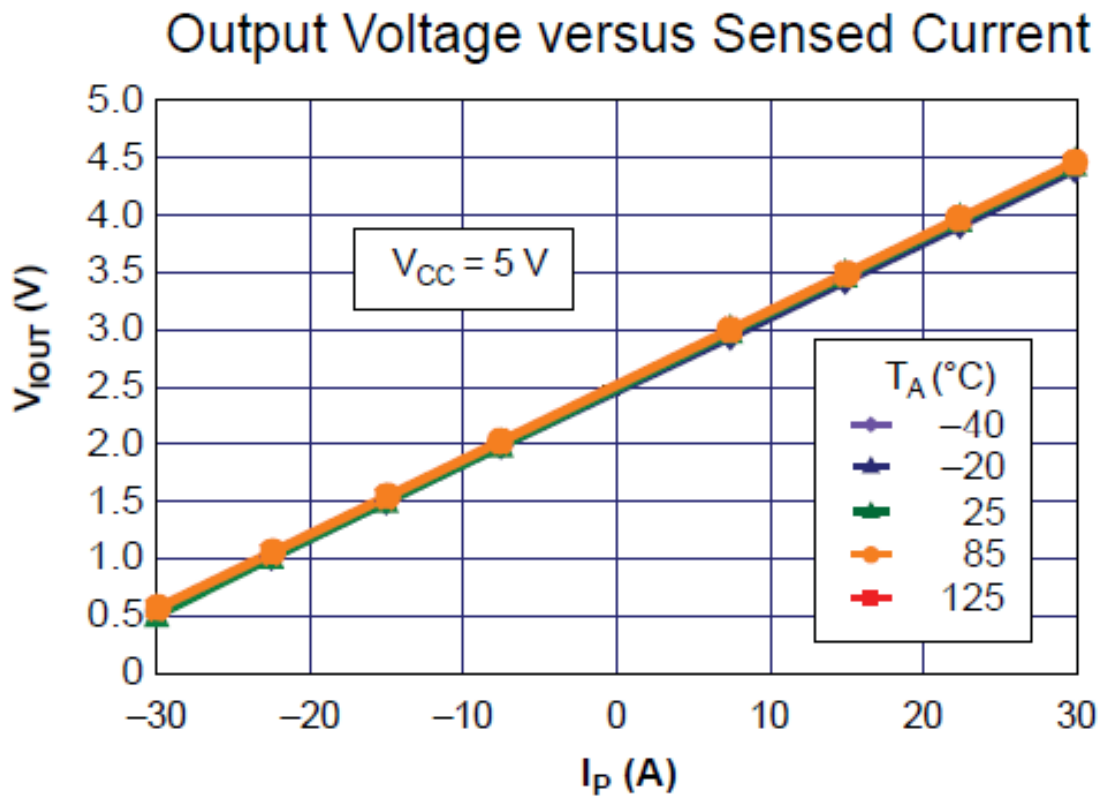
Internal reference voltages of nominally 1.1V or  $AV_{CC}$  are provided On-chip. The voltage reference may be externally decoupled at the AREF pin by a capacitor for better noise performance.

The Power Reduction ADC bit, PRADC, in "[Minimizing Power Consumption](#)" on page 42 must be disabled by writing a logical zero to enable the ADC.

The ADC converts an analog input voltage to a 10-bit digital value through successive approximation. The minimum value represents GND and the maximum value represents the voltage on the AREF pin minus 1 LSB. Optionally,  $AV_{CC}$  or an internal 1.1V reference voltage may be connected to the AREF pin by writing to the REFSn bits in the ADMUX Register. The internal voltage reference may thus be decoupled by an external capacitor at the AREF pin to improve noise immunity.

**APPENDIX D**

Graph of Output Voltage versus Sensed Current for ACS712





# PLAGIARISM CHECK RESULT

The screenshot shows the Turnitin Document Viewer interface. The main document content is centered and reads: "DC-DC CONVERTER FOR IOT DEVICES", "By Phoon Jun Hoe", "A REPORT SUBMITTED TO Universiti Tunku Abdul Rahman In fulfillment of the requirements For the degree of". The top right corner displays the Turnitin logo and a similarity score of 11%. A "Match Overview" sidebar on the right lists four matches: 1. Submitted to Universiti... (6%), 2. Toshiba Develops Wid... (3%), 3. Submitted to University... (1%), and 4. Green Energy and Tec... (1%). The browser address bar shows the URL: https://turnitin.com/dv?ts=1&oa=797796533&u=1053010869&student\_user=1&lang=en\_us&...

The screenshot shows the Turnitin student dashboard. At the top, the Turnitin logo is visible. Below it, there are navigation tabs: "Class Portfolio", "Peer Review", "My Grades", "Discussion", and "Calendar". A message box says: "Welcome to your new class homepage! From the class homepage you can see all your assignments for your class, view additional assignment information, submit your work, and access feedback for your papers." Below this is a "Class Homepage" section with instructions on how to submit and view assignments. The "Assignment Inbox: FYP2 Report" table is shown below:

Info	Dates	Similarity	
FYP 2 Report	Start: 04-Apr-2017 7:57PM Due: 05-May-2017 11:59PM Post: 12-Apr-2017 12:00AM	11%	<a href="#">Resubmit</a> <a href="#">View</a> <a href="#">Download</a>

At the bottom, there is a footer with copyright information: "Copyright © 1999 - 2017 Turnitin, LLC. All rights reserved." and various links like "Privacy Policy", "Privacy Pledge", "Terms of Service", "EU Data Protection Compliance", "Copyright Protection", "Legal FAQs", "Helpdesk", and "Research Resources".

<b>Universiti Tunku Abdul Rahman</b>			
<b>Form Title : Supervisor's Comments on Originality Report Generated by Turnitin for Submission of Final Year Project Report (for Undergraduate Programmes)</b>			
Form Number: FM-IAD-005	Rev No.: 0	Effective Date: 01/10/2013	Page No.: 1 of 1



## FACULTY OF INFORMATION AND COMMUNICATION TECHNOLOGY

<b>Full Name(s) of Candidate(s)</b>	Phoon Jun Hoe
<b>ID Number(s)</b>	1305962
<b>Programme / Course</b>	Bachelor of Information Technology (Hons) Computer Engineering
<b>Title of Final Year Project</b>	DC-DC Converter IoT Devices

<b>Similarity</b>	<b>Supervisor's Comments (Compulsory if parameters of originality exceeds the limits approved by UTAR)</b>
<b>Overall similarity index:</b> _____ %  <b>Similarity by source</b> Internet Sources: _____ % Publications: _____ % Student Papers: _____ %	
<b>Number of individual sources listed of more than 3% similarity:</b> _____	
<b>Parameters of originality required and limits approved by UTAR are as Follows:</b> (i) Overall similarity index is 20% and below, and (ii) Matching of individual sources listed must be less than 3% each, and (iii) Matching texts in continuous block must not exceed 8 words <i>Note: Parameters (i) – (ii) shall exclude quotes, bibliography and text matches which are less than 8 words.</i>	

Note Supervisor/Candidate(s) is/are required to provide softcopy of full set of the originality report to Faculty/Institute

***Based on the above results, I hereby declare that I am satisfied with the originality of the Final Year Project Report submitted by my student(s) as named above***

\_\_\_\_\_  
Signature of Supervisor

\_\_\_\_\_  
Signature of Co-Supervisor

Name: \_\_\_\_\_

Name: \_\_\_\_\_

Date: \_\_\_\_\_

Date: \_\_\_\_\_